

*Cy 1*

LOCKHEED MARTIN ENERGY RESEARCH LIBRARIES



3 4456 0515417 8

# THERMAL ANALYSIS OF THE NATIONAL RADIOACTIVE WASTE REPOSITORY: PROGRESS THROUGH MARCH 1972

R. D. Cheverton

W. D. Turner

OAK RIDGE NATIONAL LABORATORY  
CENTRAL RESEARCH LIBRARY  
DOCUMENT COLLECTION  
**LIBRARY LOAN COPY**

DO NOT TRANSFER TO ANOTHER PERSON

If you wish someone else to see this  
document, send in name with document  
and the library will arrange a loan.

UCN-7969  
(3 3-67)



## OAK RIDGE NATIONAL LABORATORY

OPERATED BY UNION CARBIDE CORPORATION • FOR THE U.S. ATOMIC ENERGY COMMISSION

Printed in the United States of America. Available from  
National Technical Information Service  
U.S. Department of Commerce  
5285 Port Royal Road, Springfield, Virginia 22151  
Price: Printed Copy \$3.00; Microfiche \$0.95

This report was prepared as an account of work sponsored by the United States Government. Neither the United States nor the United States Atomic Energy Commission, nor any of their employees, nor any of their contractors, subcontractors, or their employees, makes any warranty, express or implied, or assumes any legal liability or responsibility for the accuracy, completeness or usefulness of any information, apparatus, product or process disclosed, or represents that its use would not infringe privately owned rights.

ORNL-4789

UC-70 — Waste Disposal and Processing

Contract No. W-7405-eng-26

CHEMICAL TECHNOLOGY DIVISION

THERMAL ANALYSIS OF THE NATIONAL RADIOACTIVE WASTE REPOSITORY:  
PROGRESS THROUGH MARCH 1972

R. D. Cheverton\*  
W. D. Turner\*\*

SEPTEMBER 1972

---

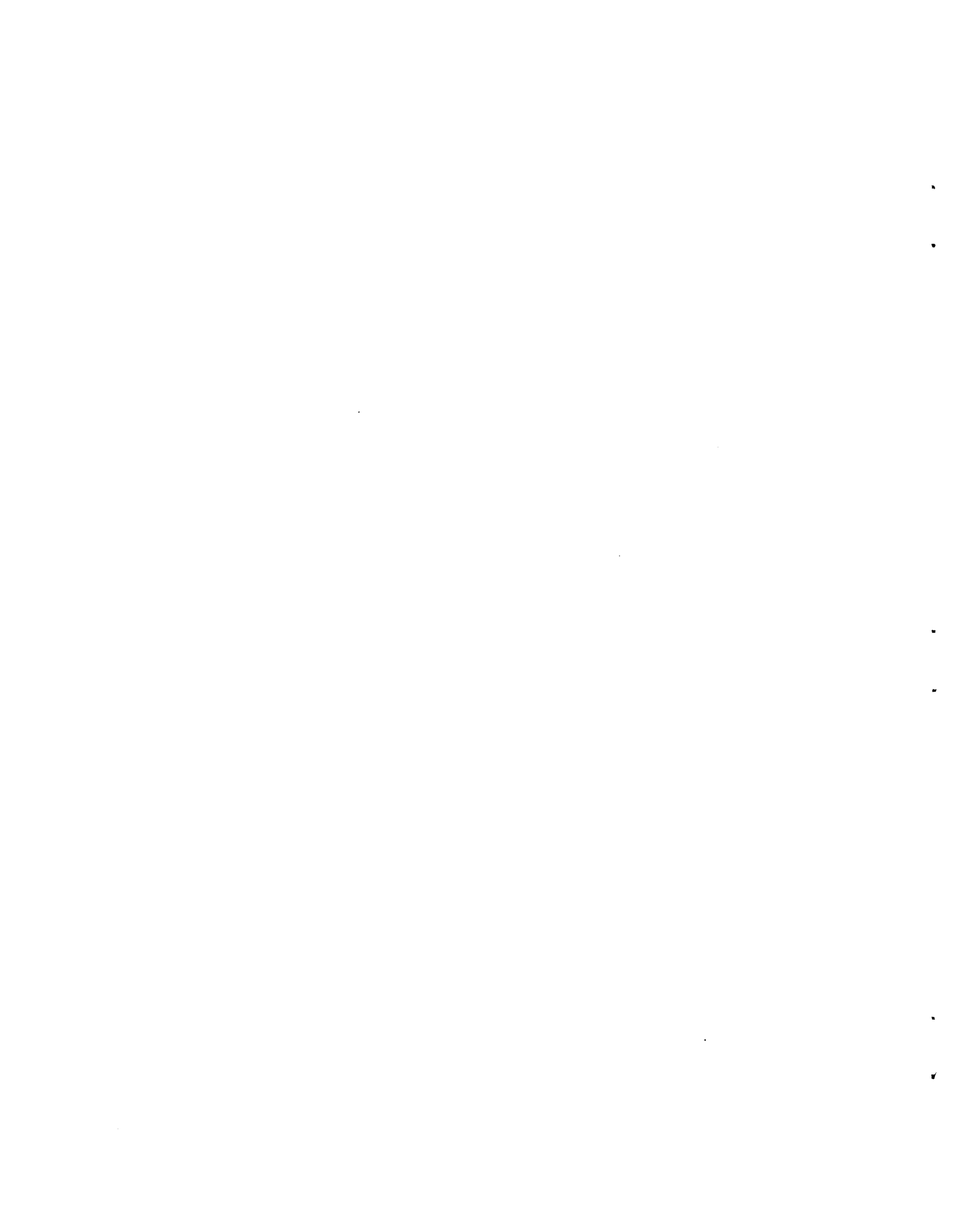
\* On loan from the Reactor Division.

\*\* Mathematics Division

OAK RIDGE NATIONAL LABORATORY  
Oak Ridge, Tennessee 37830  
operated by  
UNION CARBIDE CORPORATION  
for the  
U.S. ATOMIC ENERGY COMMISSION



3 4456 0515417 8



## CONTENTS

Abstract .....	1
1. Introduction .....	2
2. Solution of the Heat Conduction Differential Equation with Temperature-Dependent Thermal Conductivity .....	5
3. Selection of Input Parameters .....	7
3.1 Room Sizes and Waste Package Arrays for High-Level Facility .....	7
3.2 High-Level Waste Characteristics .....	8
3.3 Diameter of High-Level-Waste Container .....	10
3.4 Alpha Waste Characteristics and Burial Scheme .....	10
4. Modeling the Repository .....	13
4.1 Models for High-Level-Facility Parametric Studies .....	13
4.2 Models for High-Level-Mine Loading Sequence Studies .....	24
4.3 Model for Studying High-Level-Mine Fringe Area Effects .....	29
5. Criteria Related to Thermal Analysis .....	29
5.1 Waste Temperatures .....	29
5.2 Salt Temperatures .....	29
5.3 Temperature Increases in Freshwater Aquifers, in Mineral Deposits, and at the Earth's Surface .....	30
6. Thermal Properties .....	31
7. Results of Analysis .....	32
7.1 Parametric Analysis of the High-Level Mine .....	32
7.1.1 Permissible Loadings Based on Salt and Waste Criteria .....	35
7.1.2 Temperature of the Waste Container Surface .....	42
7.1.3 Effect of Backfill Around Waste Container .....	47

7.1.4	Power Limitations Imposed by Handling Operations Within the Repository .....	49
7.1.5	Multiple Rows of Waste Packages .....	53
7.1.6	Summary of Parametric Analysis .....	54
7.2	Temperatures Throughout the Repository .....	54
7.3	Repository Space Requirements .....	58
7.4	Diameter of the Waste Container .....	59
7.5	Temperatures in the Fringe Areas .....	62
7.6	Removal of Heat from Rooms with Ventilating Air .....	67
7.7	Cladding Hulls .....	72
7.8	Temperatures in Combustible Alpha Waste .....	73
7.9	Sensitivity of Maximum Temperatures to Loading Sequence (Phasing) .....	75
8.	References .....	80

THERMAL ANALYSIS OF THE NATIONAL RADIOACTIVE WASTE REPOSITORY:  
PROGRESS THROUGH MARCH 1972

R. D. Cheverton  
W. D. Turner

ABSTRACT

Thermal studies are continuing in connection with the burial of radioactive wastes in a salt formation similar to that at Lyons, Kansas. Parametric studies pertaining to high-level waste were recently conducted in which room size, waste package array and spacing, waste age, and power per package were variables. The objective of the studies was to aid in determining optimum burial conditions. Room widths of 15, 30, and 50 ft and waste ages of 1 to 100 years at the time of burial were considered. The previously used three-dimensional heat conduction code was revised to include the temperature dependence of the thermal conductivity, and criteria associated with limiting temperatures were modified to achieve a greater degree of consistency for the different room sizes and package arrays.

Results from the analysis show that, independent of waste age, there is an advantage in using the 15-ft room, based on Repository mining costs and gross space requirements. In connection with the latter requirements the preference for the smaller room size is restricted to the maximum permissible loading condition.

Delaying burial of the waste until about 10 years after the parent fuel is discharged from the reactor also appears to be beneficial.

The calculated maximum permissible loading per gross acre for 10-year-old waste is 6 metric tons of waste nuclides, which corresponds to 158 kW/acre at the time of burial. Considering the lowest expected thermal conductivity and permissible temperature for any of the presently anticipated wastes, and assuming a container diameter of 12 in., the maximum permissible initial (time of burial) power per waste package is 5 kW (independent of waste age). The limiting power for a 6-in.-diam container is about 3 kW.

A limitation on power per package is also imposed by various waste package handling operations within the Repository. Thermal considerations limit the power for a 6-in.-diam container to 5 kW, independent of waste age, while transporter shielding limits the power to 3.3 kW for 1-year-old waste; however, the permissible level is greater than 5 kW for wastes older than about 3.2 years.

A few calculations were made to determine the effect of varying the waste package arrays within a room. Indications thus far are that there is little difference in permissible loading surface density for one, two, and three rows in a 15-ft room and for two and three rows in a 30-ft room. It is tentatively concluded that the addition of more rows will not introduce significant changes. Thus the parametric analysis applies to very low power levels per package, accommodated by numerous rows, as well as to the higher power levels for which the calculations were made.

Calculations have also been made with regard to temperatures in the high-level repository fringe areas (adjacent rooms, corridors, shafts, etc.), and in connection with the burial of cladding hulls and alpha wastes. Neither of these cases appears to pose particularly difficult thermal problems.

---

## 1. INTRODUCTION

It is proposed that radioactive wastes such as concentrated fission products, fuel element cladding hulls, and alpha-contaminated materials be placed in salt formations beneath the earth's surface for permanent storage. Heat released from these wastes will be dissipated in the salt and surrounding geologic formations and will eventually be transferred to the atmosphere. A consequence of the subsurface heat release is an increase in the temperatures of the mined area and its environs. The temperature increases will eventually subside since the heat generation rate of the waste continuously decreases. However, thousands of years are required for the temperatures to return to normal. The design of a facility, designated as the Repository, to contain these wastes must be such that the

temperature variations will not adversely affect operational safety, containment integrity, and the environment. Results of previous studies<sup>1,2</sup> indicate that a satisfactory design can be achieved at a reasonable cost.

The design concept for the Repository calls for two separate burial areas: one for alpha waste, and another for high-level waste (fission products, actinides, and cladding hulls). The alpha waste has a power density that is about a factor of  $10^5$  less than that in the solidified high-level waste, and does not present a thermal problem of the magnitude that the high-level waste does. Thus, the thermal analysis pertains primarily to the high-level portion of the Repository, which is shown schematically in Fig. 1.1. As indicated, waste packages are buried in vertical holes beneath the floor of a room that is mined in the salt formation about 1000 ft below the earth's surface.

Previous thermal analyses<sup>2</sup> of the high-level portion of the Repository considered several different room sizes, double and single rows of waste packages, wastes of different ages, and variations in the geologic formation stratigraphy and thermal properties. It was concluded that reasonable variations in stratigraphy and thermal properties had little effect on the temperatures. However, Repository space and mining costs were found to be sensitive to room and pillar dimensions, waste package array and pitch (spacing between waste packages), loading per waste package, and age of waste at the time of burial. Thus there was a need for parametric studies that would consider these factors, and such studies are the subject of a portion of this report.

Information derived from the parametric studies is used in the overall economic analysis of waste management to determine, among other things, the optimum above ground storage time for the high-level waste

ORNL DWG 71-6182

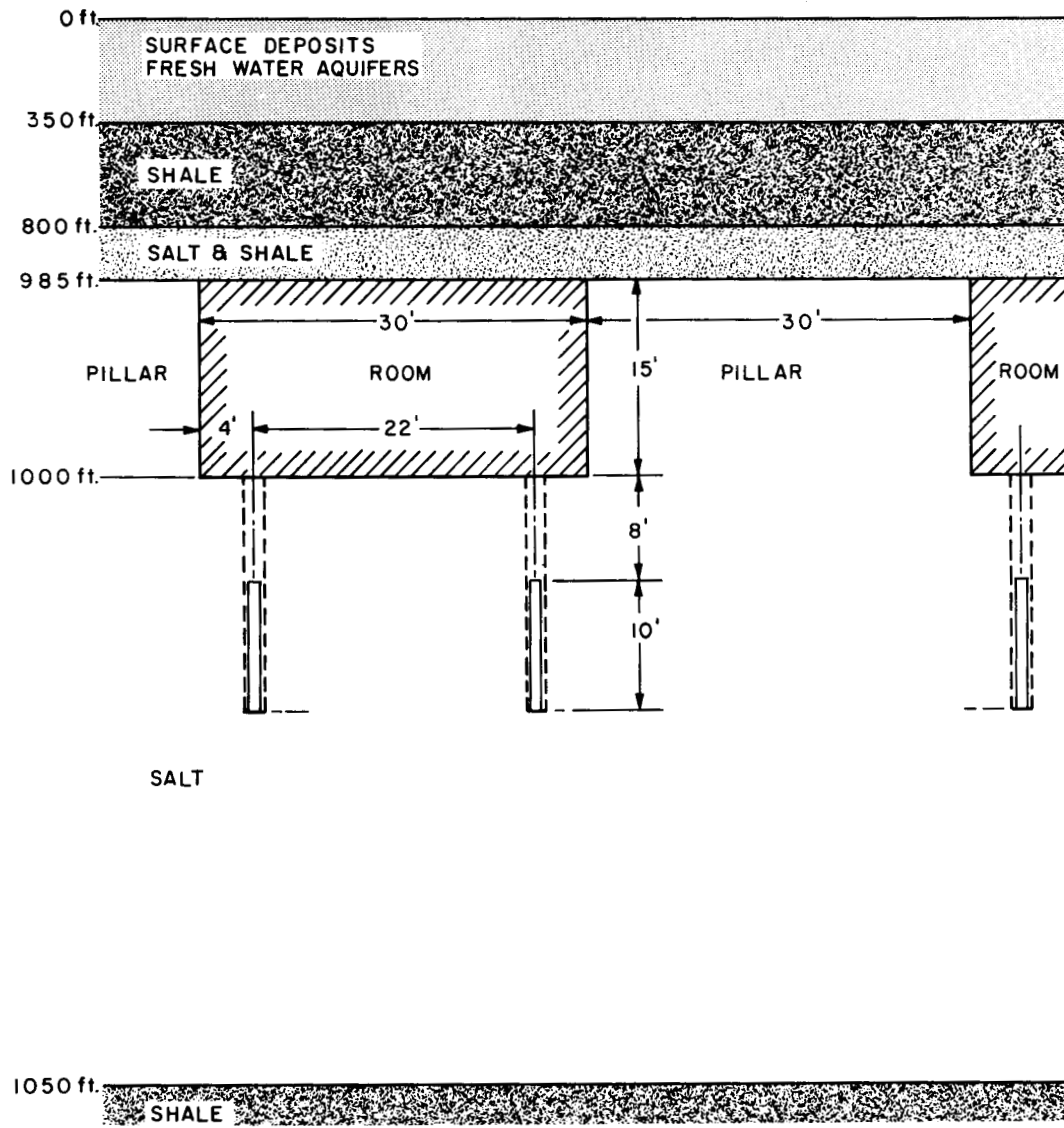


Fig. 1.1. Schematic of the Proposed Federal Radioactive Waste Repository: Vertical Cross Section of Typical High-Level Mine.

in both liquid and solid forms. Previous analyses<sup>3,4</sup> indicate that the optimum time is in the range of 3 to 10 years, assuming that the waste is solidified within 5 years of reactor discharge. Thus, for most of the calculations discussed herein, the maximum age of the waste prior to burial was assumed to be 10 years; however, a few calculations were made for 20-year-old waste, and the results were extrapolated to 100 years.

Before the parametric studies were begun, the thermal criteria were modified to achieve a greater degree of consistency between the different dimensional layouts. Furthermore, temperature dependence for the thermal conductivity of salt was incorporated in the three-dimensional heat conduction code.

In addition to the parametric studies, this report discusses temperatures in working areas adjacent to burial areas, temperatures in the alpha waste packages, temperature limitations imposed by waste package handling procedures in the high-level facility, and a three-dimensional superposition model that is being developed for mine loading sequence studies.

## 2. SOLUTION OF THE HEAT CONDUCTION DIFFERENTIAL EQUATION WITH TEMPERATURE-DEPENDENT THERMAL CONDUCTIVITY

Numerical solution of the heat conduction differential equation for 3-D(XYZ) models and with temperature-independent properties was accomplished using the alternating direction implicit procedure proposed by Douglas.<sup>5</sup> Details associated with the specific computer code developed at ORNL for the Repository studies are discussed in ref. 2. Before the recent parametric studies were begun, the ORNL code was revised to include

thermal dependence for the thermal conductivity. It is now possible to recalculate the conductivity at each node for specified time intervals that consist of one or more time steps.

The conductivity used for the time interval  $t_{m+1} - t_m$  is evaluated at the temperature

$$T_n + \left( \frac{T_n - T_{n-1}}{t_n - t_{n-1}} \right) \frac{(t_{m+1} - t_m)}{2},$$

where

$T_n$  is the last calculated temperature,

$T_n - T_{n-1}$  is the temperature change during the last time step,

$t_n - t_{n-1}$  is the last time step,

$t_{m+1} - t_m$  is the next time interval, which can consist of one or more time steps, and

$$t_m = t_n.$$

The time step and the time interval are made as large as is consistent with desired accuracy in order to reduce computer time; in principle, there is an optimum combination. For the Repository analysis, the accuracy appears to be less sensitive to the size of the time interval (effect of temperature dependence) than to the size of the time step. Trial-and-error attempts showed that, in combination with time step sizes based on the constant-thermal-property studies, the time interval could span ten time steps. Although this does not necessarily represent an optimum combination, it has been quite satisfactory for the Repository parametric studies conducted thus far. For a typical problem, the maximum difference between temperatures calculated by reevaluating the thermal conductivity for every time step and for every tenth time step was only 0.5%.

### 3. SELECTION OF INPUT PARAMETERS

#### 3.1 Room Sizes and Waste Package Arrays for High-Level Facility

Room widths of 15, 30, and 50 ft were considered in the parametric studies. The 15- and 50-ft values are specified as minimum and maximum based on waste package transporter size and maneuverability and on ceiling sag characteristics, respectively. Pillar widths for the different room sizes are based on pillar deformation analyses and, at present, are not considered to be variables. The corresponding pillar widths are 25, 30, and 50 ft.

The appropriate waste package array within a room depends upon the power per package, the size of the room, and shielding requirements. A qualitative analysis indicated that two rows in the 30- and 50-ft rooms and a single row in the 15-ft room would be best for the greater portion of the range of conditions expected. Thus, these arrays were used for most of the calculations. Furthermore, the two-row arrays were restricted to rectangular geometry because this simplified the numerical analysis. In some cases, staggering the waste packages (i.e., arranging them in triangular arrays) would improve heat transfer and shielding and will eventually be included in the analysis.

When the pitch is small compared to the transverse distance between packages, a condition encountered with low power levels, there will be thermal and shielding advantages in increasing the number of rows. Therefore, a few calculations were made with three rows in a 30-ft room and two and three rows in a 15-ft room. As an extreme in this regard, a calculation was made with the waste homogenized over a specific width of the burial zone beneath a room.

### 3.2 High-Level Waste Characteristics

Two types of high-level wastes are considered in this report:

(1) a mixture of fission products and actinides, and (2) fuel cladding hulls. The cladding hulls are considered as high-level waste because of their strong activation and because they are contaminated with fission products and actinides. In the remainder of this report, the cladding hulls will be referred to as hulls, and the fission product-actinides mixture will be referred to as high-level waste.

To date, only one type of high-level waste has been considered in the parametric analysis. It corresponds to a typical light-water reactor (LWR) fuel having an initial enrichment of 3.3%  $^{235}\text{U}$ , an average specific power of 30 MW(t)/metric ton, and a total burnup of 33,000 MWd/metric ton. It was assumed that reprocessing took place 150 days after discharge of the fuel from the reactor, that 99.5% of the uranium and plutonium was recovered during reprocessing, and that the remainder of the uranium and plutonium, plus the other actinides and fission products, were included in the solidified waste. Time-dependent compositions and heat generation rates for this waste were obtained from the computer code ORIGEN.<sup>6</sup> A compilation of nuclides and their relative heat generation rates as a function of time is presented in Table 3.1. Only those nuclides that contribute at least 1% to the total heat generation are listed in this table. The recorded total heat generation rates, however, include heat from all nuclides. It is of interest to note that essentially all of the heat during the first 200 years comes from the fission products and that the actinides make the greatest contribution in the period which follows.

Table 3.1. Nuclide Sources of Heat Generation in Fission Products and Actinides  
for a Typical LWR Waste

Nuclide	Heat Generation Rates, Relative to Grand Total at 1 Year, at Designated Times After Reprocessing at 150 Days (years):										
	1	2	5	10	20	50	100	200	500	10 <sup>3</sup>	10 <sup>4</sup>
		X10 <sup>-1</sup>	X10 <sup>-1</sup>	X10 <sup>-1</sup>	X10 <sup>-2</sup>	X10 <sup>-2</sup>	X10 <sup>-2</sup>	X10 <sup>-3</sup>	X10 <sup>-4</sup>	X10 <sup>-4</sup>	X10 <sup>-5</sup>
<sup>90</sup> Sr	0.01	0.12	0.11	0.10	0.78	0.37	0.11	0.09			
<sup>90</sup> Y	0.06	0.54	0.50	0.44	3.44	1.65	0.48	0.41			
<sup>95</sup> Nb	0.01										
<sup>99</sup> Tc											0.12
<sup>106</sup> Rh	0.25	1.28	0.16								
<sup>126</sup> Sb											0.07
<sup>134</sup> Cs	0.21	1.47	0.53	0.10							
<sup>137</sup> Cs	0.02	0.21	0.20	0.18	1.40	0.70	0.22	0.22			
<sup>137m</sup> Ba	0.05	0.48	0.45	0.40	3.16	1.58	0.50	0.49			
<sup>144</sup> Ce	0.04	0.15									
<sup>144</sup> Pr	0.30	1.24	0.09								
<sup>147</sup> Pm											
<sup>151</sup> Sm								0.05	0.05		
<sup>154</sup> Eu	0.01	0.08	0.07	0.05	0.35	0.09					
Subtotal	0.97	5.65	2.16	1.30	9.25	4.42	1.32	1.27	0.08	0.02	0.21
<sup>239</sup> Np									0.07	0.06	0.28
<sup>238</sup> Pu							0.02	0.11	0.13		
<sup>239</sup> Pu									0.07	0.08	1.64
<sup>240</sup> Pu								0.03	0.33	0.31	1.23
<sup>241</sup> Am						0.07	0.06	0.53	3.30	1.48	
<sup>243</sup> Am								0.07	0.72	0.69	3.05
<sup>242</sup> Cm	0.02										
<sup>244</sup> Cm	0.01	0.10	0.09	0.07	0.48	0.15	0.02				
Subtotal	0.03	0.15	0.10	0.08	0.61	0.27	0.12	0.78	4.64	2.63	6.26
Total	1	5.81	2.26	1.39	9.85	4.69	1.44	2.04	4.72	2.66	6.47

A curve of relative heat generation vs time is shown in Fig. 3.1.

The thermal conductivity and the maximum permissible temperature for the waste (i.e.,  $0.25 \text{ Btu hr}^{-1} \text{ ft}^{-1} (\text{°F})^{-1}$  and  $1100\text{°F}$ , respectively) were the least expected nominal values for any of the anticipated solidified wastes. For many of the calculated cases, the waste temperature was limiting; thus there is some incentive for improving the thermal properties of the waste.

The hulls that were considered in the calculations were assumed to have been discharged from the same LWR and to have been exposed to the same operating conditions as the high-level waste discussed in this report.<sup>7</sup> It was assumed that the zircaloy hulls were contaminated with 0.1% of the high-level waste. Heat generation rate as a function of time for this "waste" is shown in Fig. 3.1. The burial scheme for the hulls was assumed to be the same as that for the high-level waste.

### 3.3 Diameter of High-Level-Waste Container

The high-level-waste container was assumed to have a 6-in. diameter for the parametric analysis. Increasing the diameter tends to reduce temperatures in the waste and in the salt adjacent to the container. Although small, this effect will be considered in greater detail in a future analysis.

### 3.4 Alpha Waste Characteristics and Burial Scheme

The analysis of the alpha facility was based on a typical alpha waste composition consisting of 1%  $^{238}\text{Pu}$ , 60%  $^{239}\text{Pu}$ , 24%  $^{240}\text{Pu}$ , 11%  $^{241}\text{Pu}$ , and 4%  $^{242}\text{Pu}$ . The heat generation characteristics for this waste are shown in Table 3.2.

ORNL-DWG 72-6995

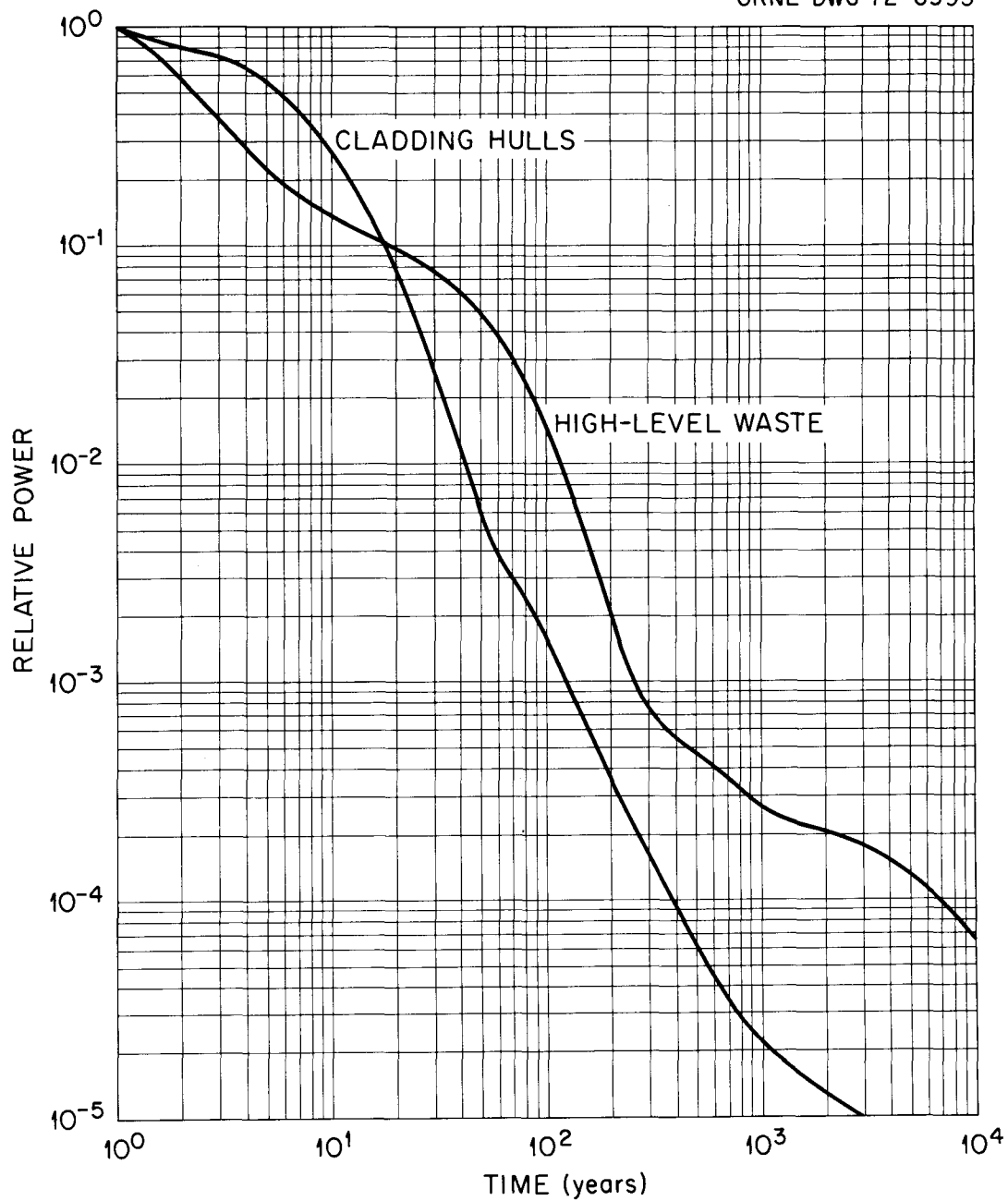


Fig. 3.1. Relative Thermal Power of Typical High-Level Waste and Cladding Hulls from a Light Water Reactor.

Table 3.2. Heat Generation Rate of Typical Alpha Waste  
as a Function of Time

Time (yr)	Power <sup>α</sup> (W)	Time from Mine Closure = Total Time - 26 years	Power (W)
0	0	30	6.55 X 10 <sup>5</sup>
1	7.97 X 10 <sup>2</sup>	1 X 10 <sup>2</sup>	6.13 X 10 <sup>5</sup>
2	3.23 X 10 <sup>3</sup>	3 X 10 <sup>2</sup>	4.28 X 10 <sup>5</sup>
3	5.80 X 10 <sup>2</sup>	1 X 10 <sup>3</sup>	1.99 X 10 <sup>5</sup>
4	8.49 X 10 <sup>3</sup>	3 X 10 <sup>3</sup>	9.08 X 10 <sup>4</sup>
5	1.13 X 10 <sup>4</sup>	1 X 10 <sup>4</sup>	5.58 X 10 <sup>4</sup>
6	1.42 X 10 <sup>4</sup>	3 X 10 <sup>4</sup>	2.20 X 10 <sup>4</sup>
7	1.96 X 10 <sup>4</sup>	1 X 10 <sup>5</sup>	3.25 X 10 <sup>3</sup>
8	2.69 X 10 <sup>4</sup>	3 X 10 <sup>5</sup>	8.74 X 10 <sup>2</sup>
9	3.44 X 10 <sup>4</sup>	1 X 10 <sup>6</sup>	6.20 X 10 <sup>2</sup>
10	4.39 X 10 <sup>4</sup>	3 X 10 <sup>6</sup>	2.89 X 10 <sup>2</sup>
11	5.37 X 10 <sup>4</sup>	1 X 10 <sup>7</sup>	5.04 X 10
12	6.78 X 10 <sup>4</sup>	3 X 10 <sup>7</sup>	1.89 X 10
13	8.76 X 10 <sup>4</sup>		
14	1.14 X 10 <sup>5</sup>		
15	1.41 X 10 <sup>5</sup>		
16	1.70 X 10 <sup>5</sup>		
17	1.99 X 10 <sup>5</sup>		
18	2.29 X 10 <sup>5</sup>		
19	2.61 X 10 <sup>5</sup>		
20	2.92 X 10 <sup>5</sup>		
21	3.25 X 10 <sup>5</sup>		
22	3.59 X 10 <sup>5</sup>		
23	3.93 X 10 <sup>5</sup>		
24	4.28 X 10 <sup>5</sup>		
25	4.63 X 10 <sup>5</sup>		
26	4.76 X 10 <sup>5</sup>		

<sup>α</sup> Total power of all alpha waste considered for burial in  
the Repository.

It has been estimated<sup>8</sup> that  $1.53 \times 10^8$  ft<sup>3</sup> (prior to compaction) of alpha waste will be accommodated in the Repository by the year 2000. If the specified compaction schedule is followed, the gross space required for the waste will be 180 acres. The heat generation input used in the thermal analysis was based on these quantities and on an average plutonium concentration in the waste, prior to compaction, of 0.25 g/ft<sup>3</sup>. It was further assumed that the waste packages would be placed adjacent to each other and stacked 10 ft high in rooms that are about 1000 ft below the earth's surface.

#### 4. MODELING THE REPOSITORY

##### 4.1 Models for High-Level-Facility Parametric Studies

The two- and three-dimensional models used for most of the parametric studies are essentially the same as those discussed in ref. 2. Boundaries on the latest two-dimensional model are extended to permit consideration of longer times after burial. In the latest three-dimensional model the pitch is a variable, and salt subregions are removed, consistent with the application of temperature-dependent thermal properties for the salt. The 2-D(RZ) model is shown in Fig. 4.1; 3-D(XYZ) models for the 15-, 30-, and 50-ft rooms are shown in Figs. 4.2, 4.3, and 4.4, respectively. Additional detailed information pertaining to these models is given in Tables 4.1 - 4.4.

An additional 2-D(RZ) model, which simulates a high-level facility with an adjacent alpha facility, is shown in Fig. 4.5 and is further described in Table 4.5. Additional 3-D(XYZ) models included different

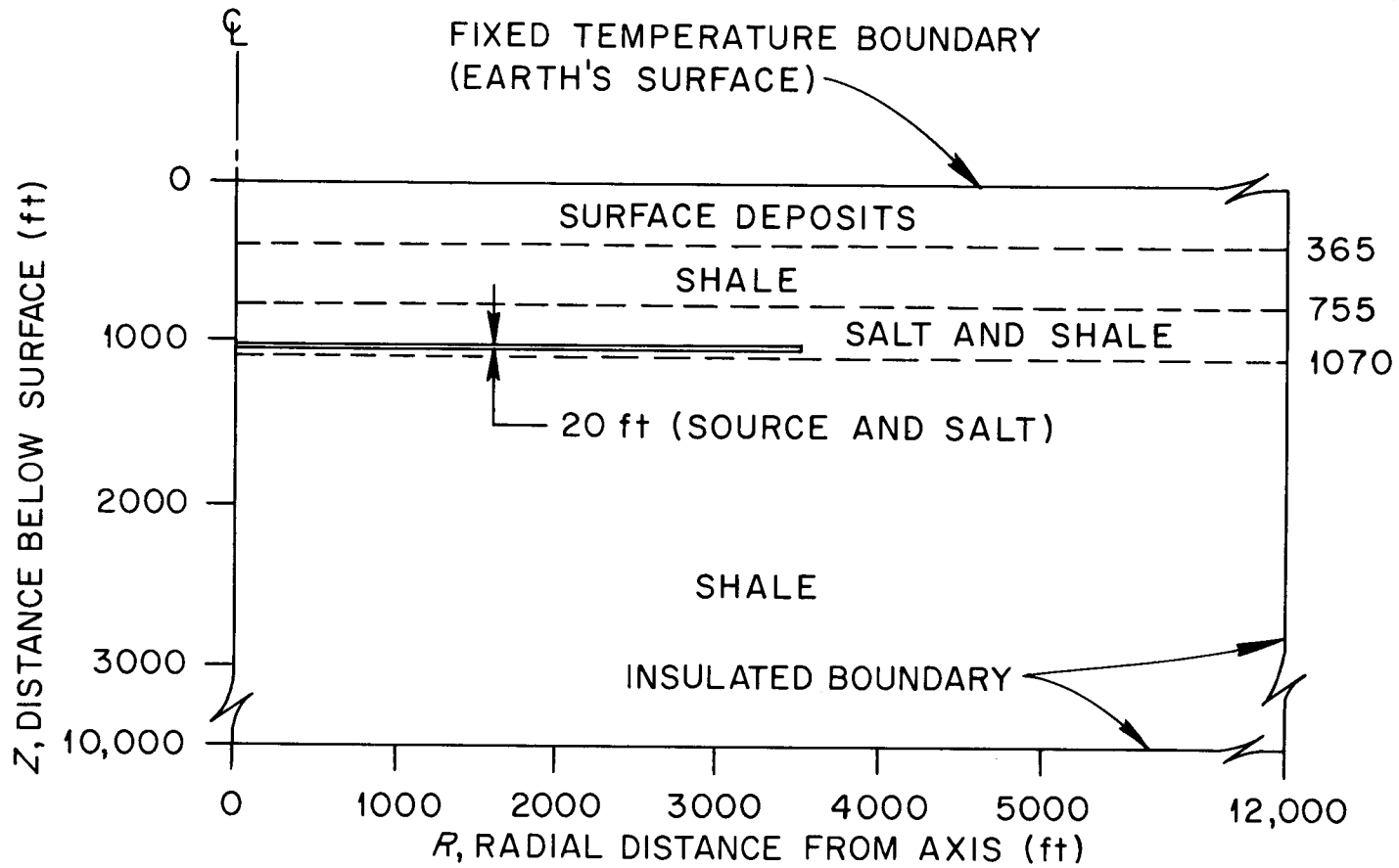


Fig. 4.1. Two-Dimensional Cylindrical Model of the High-Level Mine.

ORNL-DWG 71-9511A

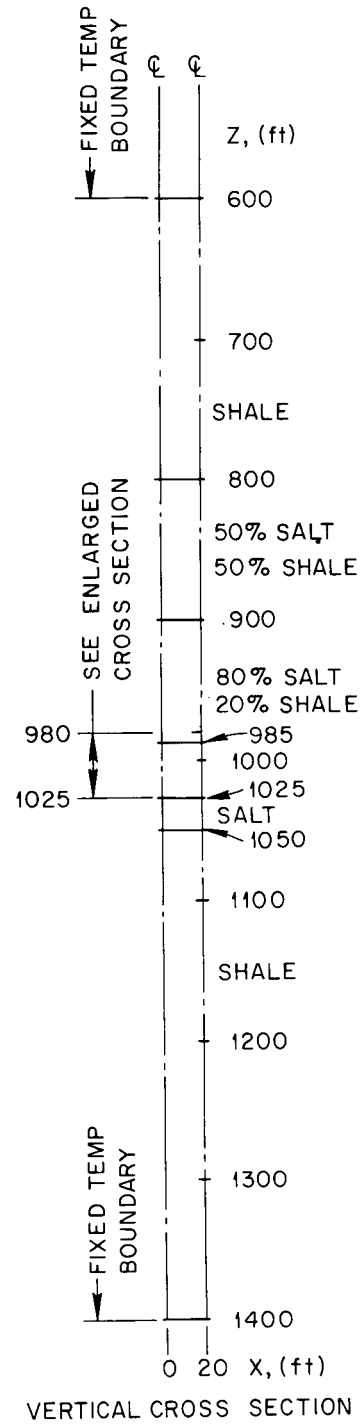
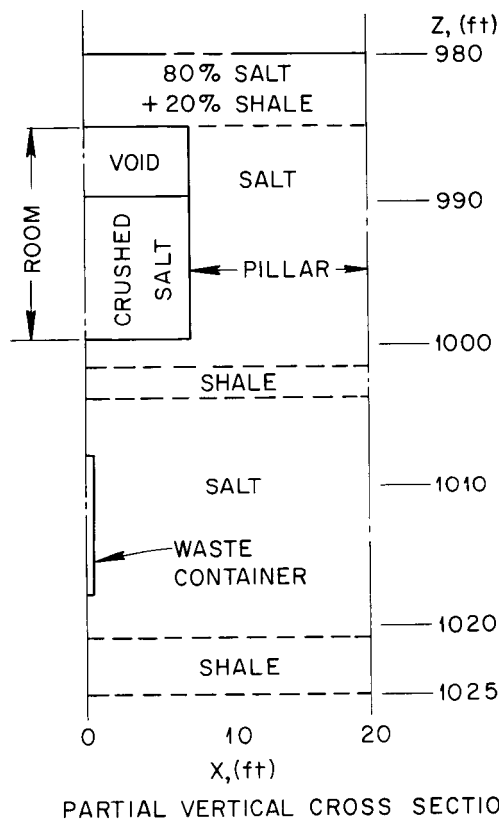
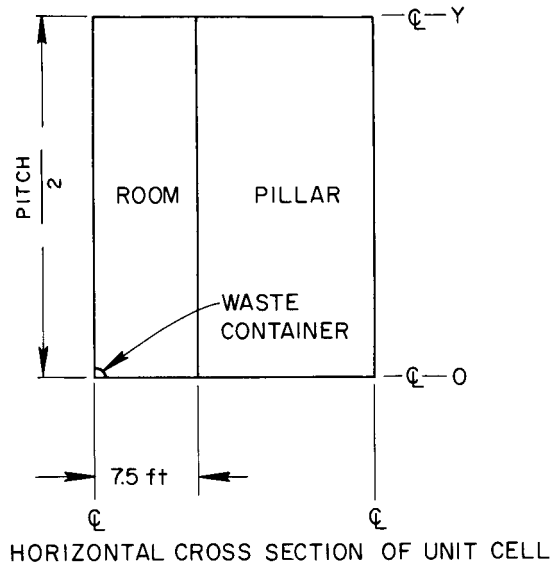


Fig. 4.2. Three-Dimensional Model of a Unit Cell of the High-Level Mine: 15-ft Room.

ORNL-DWG 71-2895A

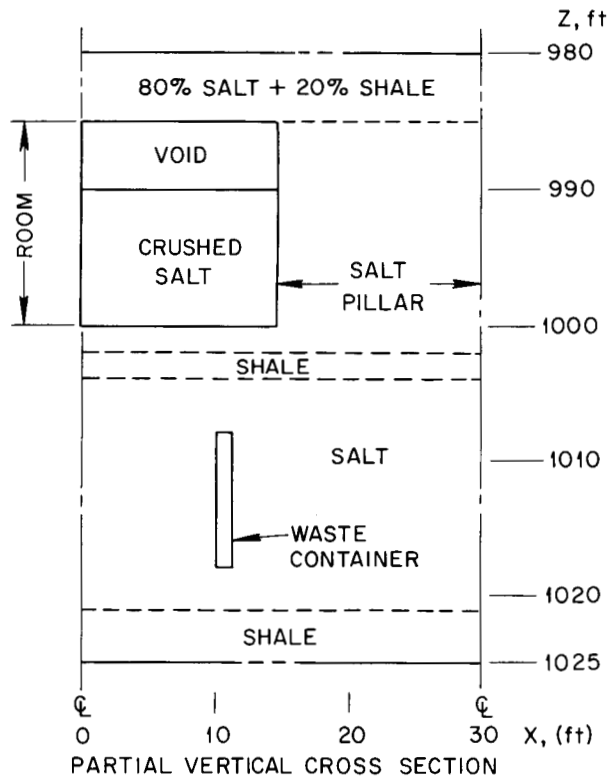
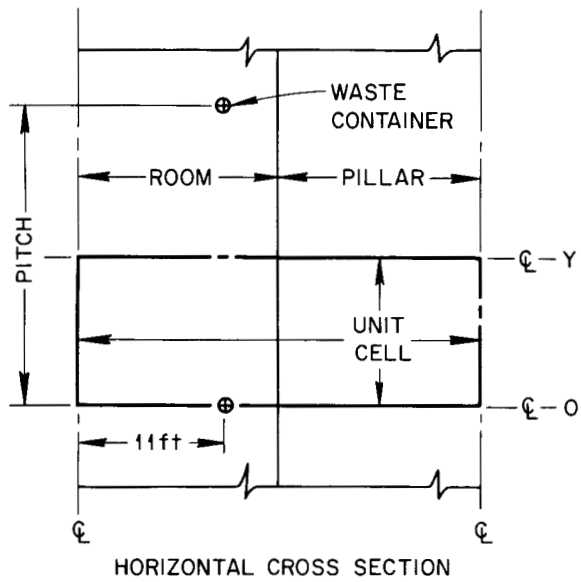


Fig. 4.3 Three-Dimensional Model of a Unit Cell of the High-Level

Mine: 30-ft Room.

ORNL-DWG 71-9503A

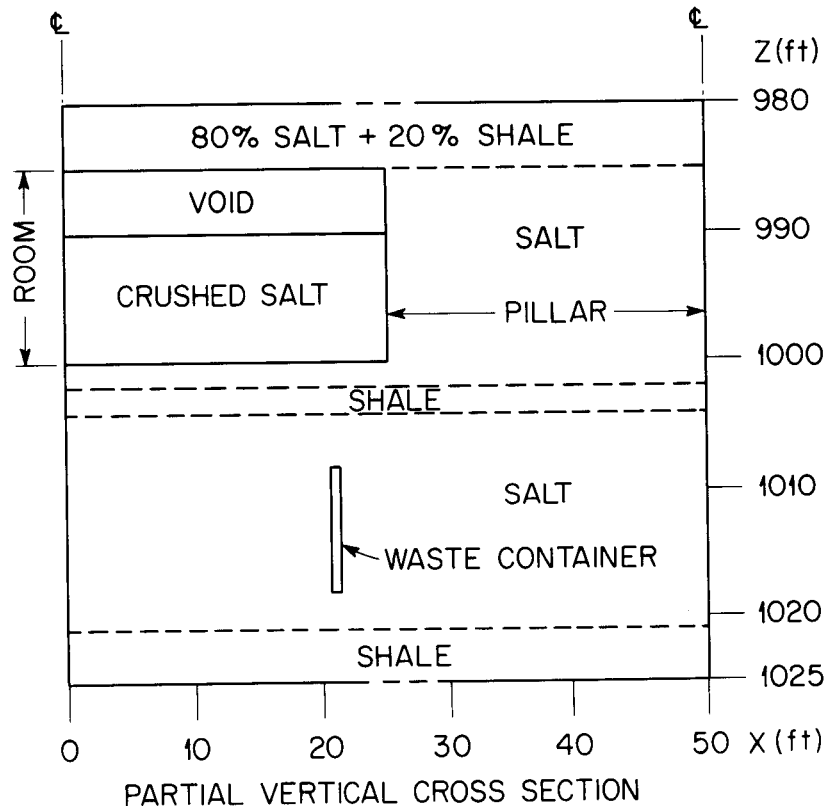
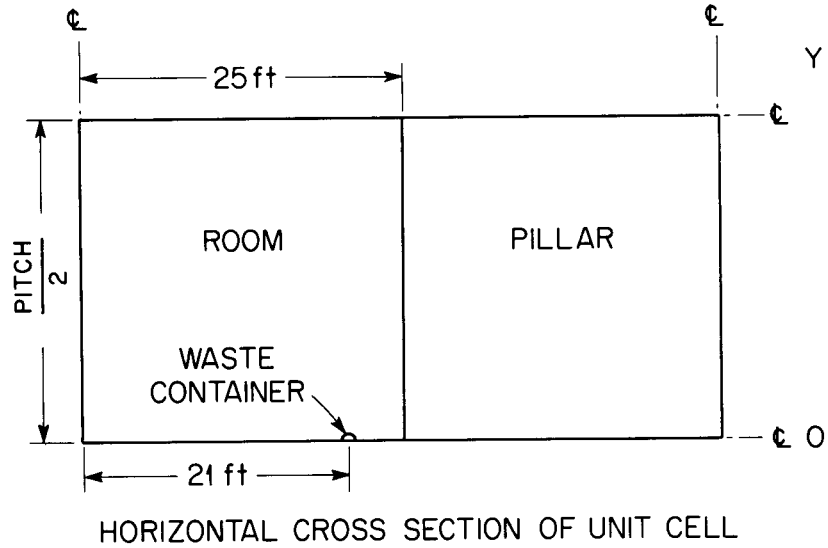


Fig. 4.4. Three-Dimensional Model of a Unit Cell of the High-Level

Mine: 50-ft Room.

Table 4.1. Description of Two-Dimensional Cylindrical Model

## A. Region Definition

Region No.	Material No. <sup>a</sup>	Inner R <sup>b</sup>	Outer R <sup>b</sup>	Upper Z <sup>b</sup>	Lower Z <sup>b</sup>
1	1	0	12,000	0	365
2	2	0	12,000	365	755
3	3	0	12,000	755	1000
4 <sup>c</sup>	4	0	3500	1000	1020
5	3	3500	12,000	1000	1020
6	3	0	12,000	1020	1070
7	2	0	12,000	1070	10,000

## B. Grid Line Locations

Grid Line Index (I, J, or K)	R <sup>b</sup>	Z <sup>b</sup>
1	0	0
2	500	100
3	1000	200
4	1500	300
5	2000	365
6	2500	400
7	3000	500
8	3500	600
9	3750	700
10	4000	755
11	4250	800
12	4500	850
13	4750	900
14	5000	925
15	5250	950
16	5500	975
17	5750	1000
18	6000	1020
19	6250	1045
20	6500	1070
21	7000	1100
22	7500	1150
23	8000	1200
24	8500	1250
25	9000	1300
26	9500	1400
27	10,000	1500
28	10,500	1600
29	11,000	1800
30	11,500	2000
31	12,000	2200
32		2400
33		2600
34		2800
35		3000
36		3250
37		3500
38		4000
39		4500
40		5000
41		5500
42		6000
43		7000
44		8000
45		9000
46		10,000

<sup>a</sup> See Table 6.2 for the names and thermal properties of the materials.

<sup>b</sup> Dimensions are given in feet.

<sup>c</sup> Heat generation occurs in this region.

Table 4.2. Description of Three-Dimensional Model for a 15-ft Room in the Repository

## A. Region Definition

Region No.	Material <sup>a</sup> No.	Left X <sup>b</sup>	Right X <sup>b</sup>	Front Y <sup>b</sup>	Back Y <sup>b</sup> for			Top Z <sup>b</sup>	Bottom Z <sup>b</sup>
					Pitch (ft) of:				
					10	30	50		
1	10	0	20	0	5	15	25	600	800
2	7	0	20	0	5	15	25	800	900
3	6	0	20	0	5	15	25	900	985
4	8	0	7.5	0	5	15	25	990	1000
5	5	7.5	20	0	5	15	25	985	1000
6	5	0	20	0	5	15	25	1000	1002
7	10	0	20	0	5	15	25	1002	1004
8	5	0	20	0	5	15	25	1004	1008
9	5	0	20	0	5	15	25	1018	1021
10	10	0	20	0	5	15	25	1021	1025
11	5	0	20	0	5	15	25	1025	1050
12	10	0	20	0	5	15	25	1050	1400
13	5	0.25	20	0	5	15	25	1008	1018
14	5	0	0.25	0.25	5	15	25	1008	1018
15 <sup>c</sup>	9	0	0.25	0	0.25	0.25	0.25	1008	1018

## B. Grid Line Locations

Grid Line Index (I, J, or K)	X <sup>b</sup>	Y <sup>b</sup>			Z <sup>b</sup>
		Pitch (ft)			
		10	30	50	
1	0	0	0	0	600
2	0.25	0.25	0.25	0.25	700
3	0.75	0.75	0.75	0.75	800
4	1.5	1.5	1.5	1.5	900
5	3	3	3	3	950
6	5	5	5	5	980
7	7.5	7.5	7.5	7.5	985
8	10	10	10	10	990
9	15	15	15	15	995
10	20	20	20	20	1000
11			25	25	1002
12					1004
13					1006
14					1008
15					1010.5
16					1013
17					1015.5
18					1018
19					1021
20					1025
21					1050
22					1100
23					1200
24					1300
25					1400

<sup>a</sup> See Table 6.2 for the names and thermal properties of the materials.<sup>b</sup> Dimensions are given in feet.<sup>c</sup> Heat generation occurs in this region.

Table 4.3. Description of Three Dimensional Model for a 30-ft Room in the Repository

## A. Region Description

Region No.	Material <sup>a</sup> No.	Left X <sup>b</sup>	Right X <sup>b</sup>	Front Y <sup>b</sup>	Back Y <sup>b</sup> for			Top Z <sup>b</sup>	Bottom Z <sup>b</sup>
					Pitch (ft) of:				
					10	30	50		
1	10	0	30	0	5	15	25	600	800
2	7	0	30	0	5	15	25	800	900
3	6	0	30	0	5	15	25	900	985
4	8	0	15	0	5	15	25	990	1000
5	5	15	30	0	5	15	25	985	1000
6	5	0	30	0	5	15	25	1000	1002
7	10	0	30	0	5	15	25	1002	1004
8	5	0	30	0	5	15	25	1004	1008
9	5	0	30	0	5	15	25	1018	1021
10	10	0	30	0	5	15	25	1021	1025
11	5	0	30	0	5	15	25	1025	1050
12	10	0	30	0	5	15	25	1050	1400
13	5	0	10.75	0	5	15	25	1008	1018
14	5	10.75	11.25	0.25	5	15	25	1008	1018
15	5	11.25	30	0	5	15	25	1008	1018
16 <sup>c</sup>	9	10.75	11.25	0	0.25	0.25	0.25	1008	1018

## B. Grid Line Locations

Grid Line Index (I, J, or K)	X <sup>b</sup>	Y <sup>b</sup> for			Z <sup>b</sup>
		Pitch (ft) of:			
		10	30	50	
1	0	0	0	0	600
2	5	0.25	0.25	0.25	700
3	8	0.75	0.75	0.75	800
4	9.5	1.5	1.5	1.5	900
5	10.25	3	3	3	950
6	10.75	5	5	5	980
7	11.25		7.5	7.5	985
8	11.75		10	10	990
9	12.5		15	15	995
10	14			20	1000
11	15			25	1002
12	17.5				1004
13	20				1006
14	25				1008
15	30				1010.5
16					1013
17					1015.5
18					1018
19					1021
20					1025
21					1050
22					1100
23					1200
24					1300
25					1400

<sup>a</sup>See Table 6.2 for the names and thermal properties of the materials.

<sup>b</sup>Dimensions are given in feet.

<sup>c</sup>Heat generation occurs in this region.

Table 4.4. Description of Three-Dimensional Model for a  
50-ft Room in the Repository

A. Region Description

Region No.	Material <sup>a</sup> No.	Left X <sup>b</sup>	Right X <sup>b</sup>	Front Y <sup>b</sup>	Back Y <sup>b</sup> for			Top Z <sup>b</sup>	Bottom Z <sup>b</sup>
					Pitch (ft) of:				
					10	30	50		
1	10	0	50	0	5	15	25	600	800
2	7	0	50	0	5	15	25	800	900
3	6	0	50	0	5	15	25	900	985
4	8	0	25	0	5	15	25	990	1000
5	5	25	50	0	5	15	25	985	1000
6	5	0	50	0	5	15	25	1000	1002
7	10	0	50	0	5	15	25	1002	1004
8	5	0	50	0	5	15	25	1004	1008
9	5	0	50	0	5	15	25	1018	1021
10	10	0	50	0	5	15	25	1021	1025
11	5	0	50	0	5	15	25	1025	1050
12	10	0	50	0	5	15	25	1050	1400
13	5	0	20.75	0	5	15	25	1008	1018
14	5	20.75	21.25	0.25	5	15	25	1008	1018
15	5	21.25	50	0	5	15	25	1008	1018
16 <sup>c</sup>	9	0	0.25	0	0.25	0.25	0.25	1008	1018

B. Grid Line Locations

Grid Line Index (I, J, or K)	X <sup>b</sup>	Y <sup>b</sup> for			Z <sup>b</sup>
		Pitch (ft) of:			
		10	30	50	
1	0	0	0	0	600
2	5	0.25	0.25	0.25	700
3	10	0.75	0.75	0.75	800
4	15	1.5	1.5	1.5	900
5	18	3	3	3	950
6	19.5	5	5	5	980
7	20.25		7.5	7.5	985
8	20.75		10	10	990
9	21.25		15	15	995
10	21.75			20	1000
11	22.5			25	1002
12	24				1004
13	25				1006
14	27.5				1008
15	30				1010.5
16	35				1013
17	40				1015.5
18	50				1018
19					1021
20					1025
21					1050
22					1100
23					1200
24					1300
25					1400

<sup>a</sup>See Table 6.2 for the names and thermal properties of the materials.

<sup>b</sup>Dimensions are given in feet.

<sup>c</sup>Heat generation occurs in this region.

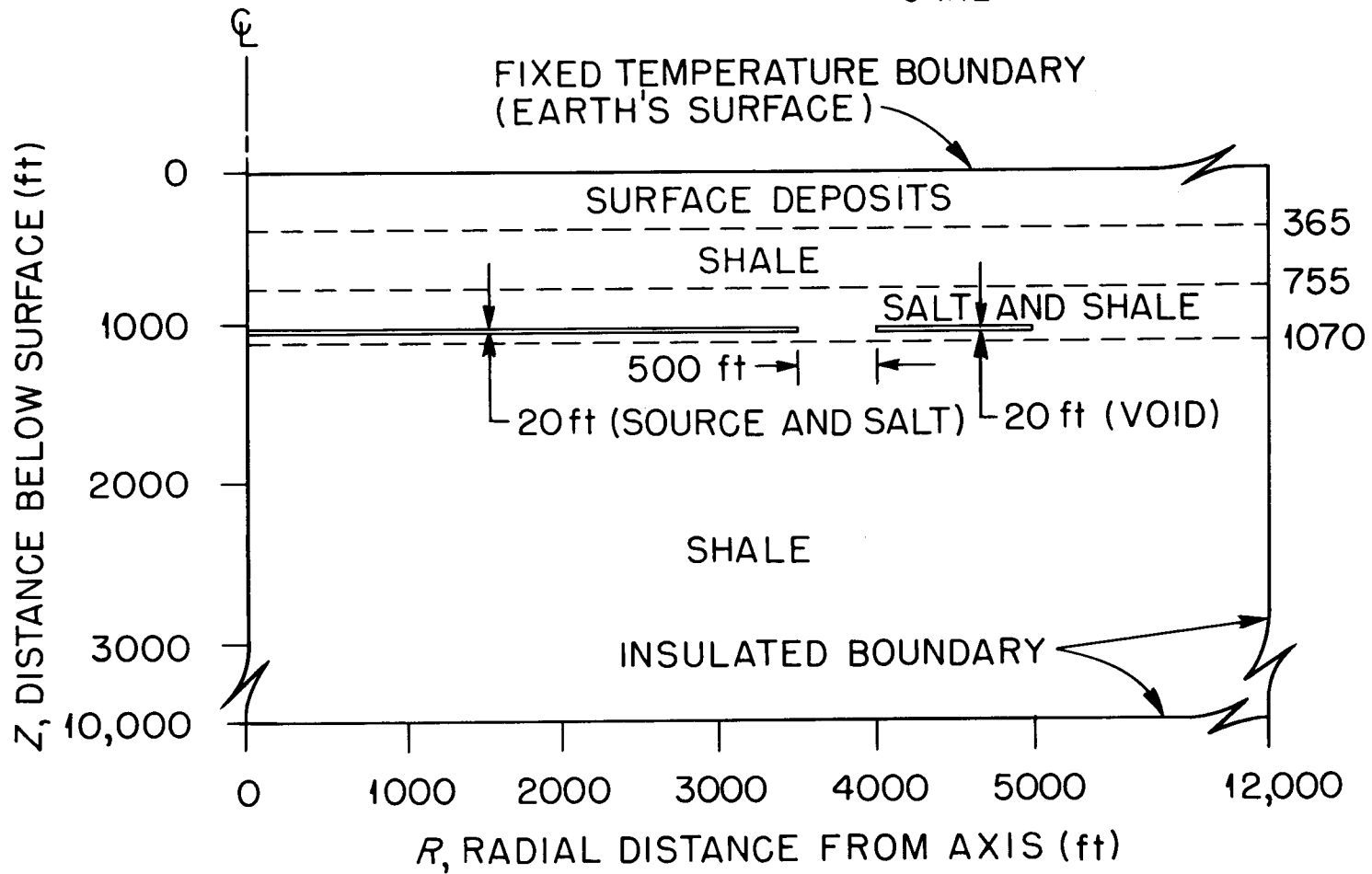


Fig. 4.5. Two-Dimensional Cylindrical Model of the High-Level Mine and Adjacent Alpha Facility.

Table 4.5. Description of Two-Dimensional Cylindrical Model  
Simulating High-Level Waste Repository with  
Adjacent Alpha Facility

A. Region Definition

Region No.	Material No. <sup>a</sup>	Inner R <sup>b</sup>	Outer R <sup>b</sup>	Upper Z <sup>b</sup>	Lower Z <sup>b</sup>
1	1	0	12,000	0	365
2	2	0	12,000	365	755
3	3	0	12,000	755	1000
4 <sup>c</sup>	4	0	3500	1000	1020
5	3	3500	4000	1000	1020
6	3	5000	12,000	1000	1020
7	3	0	12,000	1020	1070
8	2	0	12,000	1070	10,000

B. Grid Line Locations

Grid Line Index (I, J, or K)	R <sup>b</sup>	Z <sup>b</sup>
1	0	0
2	500	100
3	1000	200
4	1500	300
5	2000	365
6	2500	400
7	3000	500
8	3250	600
9	3300	700
10	3350	755
11	3400	800
12	3450	850
13	3500	900
14	3550	925
15	3600	950
16	3650	975
17	3700	1000
18	3750	1020
19	3800	1045
20	3850	1070
21	3900	1100
22	3950	1150
23	4000	1200
24	4250	1250
25	4500	1300
26	4750	1400
27	5000	1500
28	5500	1600
29	6000	1800
30	6500	2000
31	7000	2200
32	7500	2400
33	8000	2600
34	8500	2800
35	9000	3000
36	9500	3250
37	10,000	3500
38	12,000	4000
39		4500
40		5000
41		5500
42		6000
43		7000
44		8000
45		9000
46		10,000

<sup>a</sup>See Table 6.2 for the names and thermal properties of the materials.

<sup>b</sup>Dimensions are given in feet.

<sup>c</sup>Heat generation occurs in this region.

high-level-package arrays for the 15- and 30-ft rooms, including a homogenized source zone. These arrays are shown in Fig. 4.6.

The use of rectangular geometry (XYZ) in the 3-D models makes it necessary to represent the cylindrical waste package with a rectangular parallelepiped having a square cross section normal to the long axis. In each case, the sides of the square cross section were tangent to the cylindrical surface of the waste container. Thus, the surface area and the volume of the parallelepiped were greater by a factor of  $4/\pi$  than for the cylinder. To determine the effect this had on the calculated surface temperatures 2-D(XY) and 1-D(R) comparison calculations were made. The results indicated that, when the cylinder and the parallelepiped contain the same power per unit length, the surface temperatures agree to within about 3%.

#### 4.2 Models for High-Level-Mine Loading Sequence Studies

To facilitate the study of mine loading sequence effects on temperature distributions, two superposition models are being developed. One of them, shown in Fig. 4.7 and further described in Table 4.6, depicts a unit cell consisting of a square slab source region and a square room-pillar-corridor region embedded in an effectively infinite extent of the formation as considered in the other 3-D(XYZ) models. Three of these unit cells, placed in series so that the source and room-pillar-corridor regions are continuous, make up a rectangular section of the Repository, one end of which ties into the main corridor. Sections are placed side by side on both sides of a main corridor to make up the entire mined portion of the Repository. The horizontal dimensions

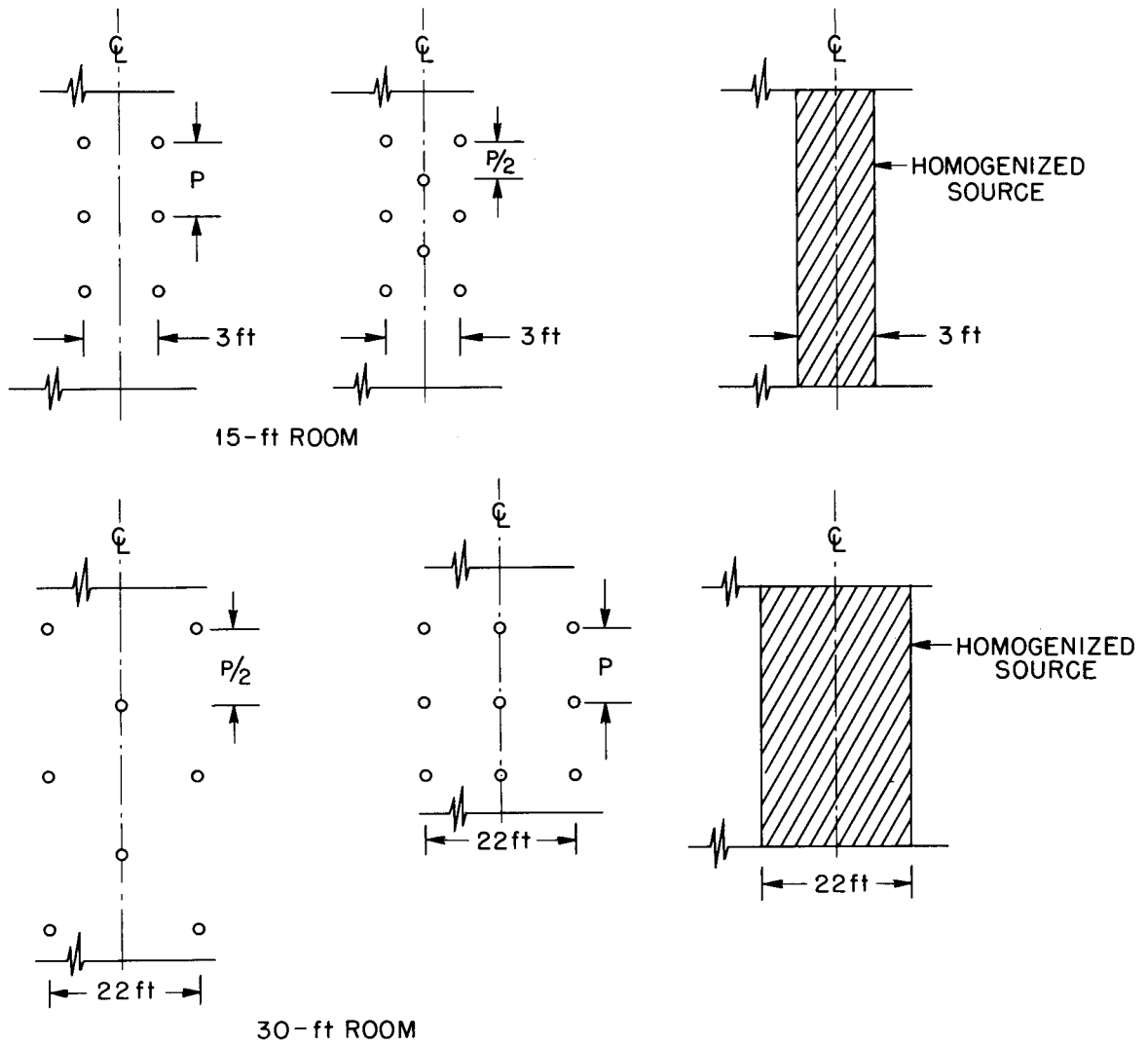


Fig. 4.6. Additional Arrays for the 3-D(XYZ) Models of the High-Level Mine.

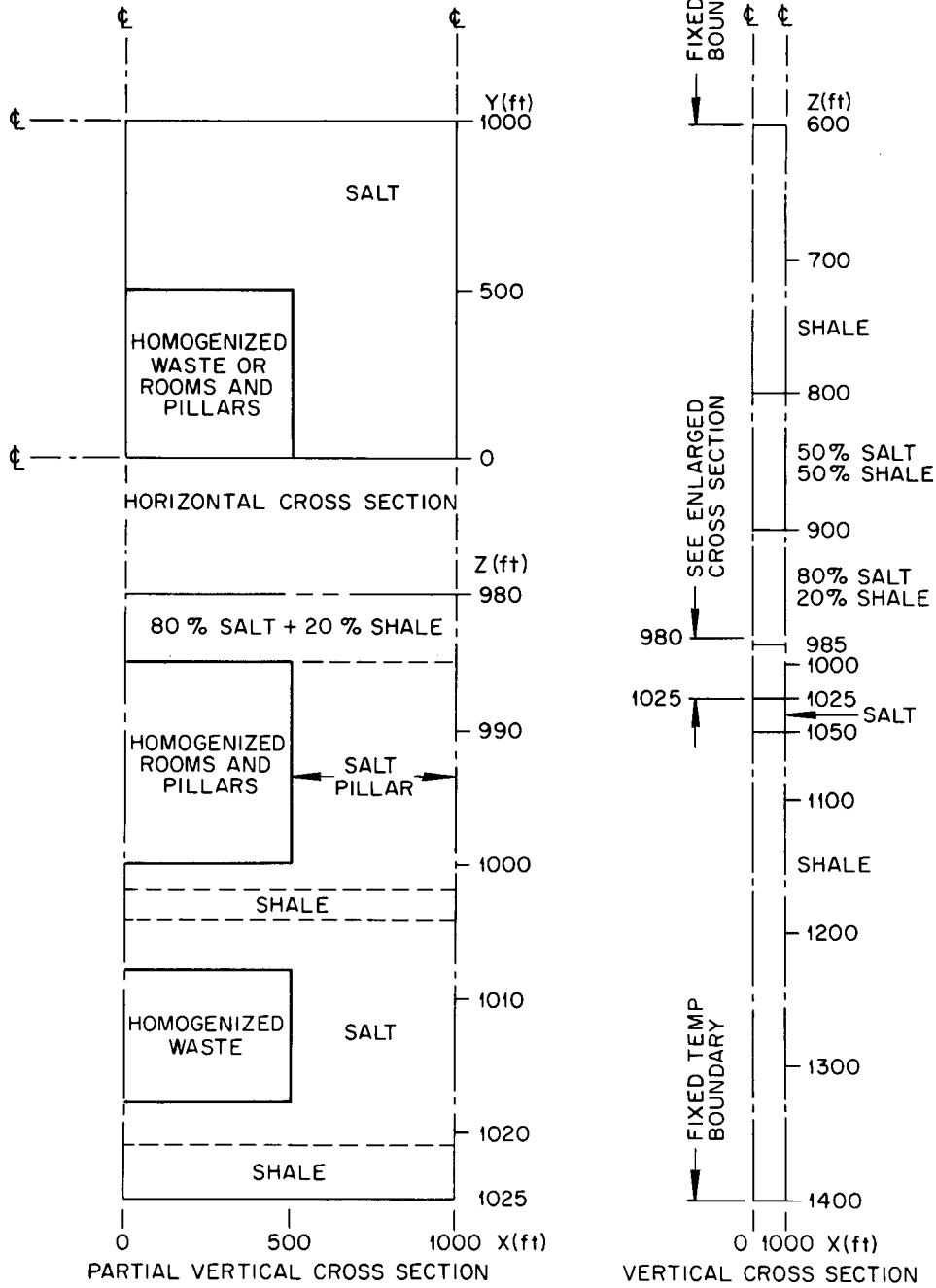


Fig. 4.7. Three-Dimensional Superposition Model for the High-Level

Mine.

Table 4.6. Description of 3-D (XYZ) Superposition Model for the High-Level Mine

A. Region Definition

Region No.	Material <sup>a</sup> No.	Left X <sup>b</sup>	Right X <sup>b</sup>	Front Y <sup>b</sup>	Back Y <sup>b</sup>	Top Z <sup>b</sup>	Bottom Z <sup>b</sup>
1	10	0	1000	0	1000	600	800
2	7	0	1000	0	1000	800	900
3	6	0	1000	0	1000	900	985
4	11	0	500	0	500	985	1000
5	5	0	500	500	1000	985	1000
6	5	500	1000	0	1000	985	1000
7	5	0	1000	0	1000	1000	1002
8	10	0	1000	0	1000	1002	1004
9	5	0	1000	0	1000	1004	1008
10 <sup>c</sup>	5	0	500	0	500	1008	1018
11	5	0	500	500	1000	1008	1018
12	5	500	1000	0	1000	1008	1018
13	5	0	1000	0	1000	1018	1021
14	10	0	1000	0	1000	1021	1025
15	5	0	1000	0	1000	1025	1050
16	10	0	1000	0	1000	1050	1400

B. Grid Line Locations

Grid Line Index (I, J, or K)	X <sup>b</sup>	Y <sup>b</sup>	Z <sup>b</sup>
1	0	0	600
2	200	200	650
3	300	300	700
4	400	400	750
5	450	450	800
6	500	500	850
7	550	550	900
8	600	600	925
9	700	700	950
10	800	800	962.5
11	1000	1000	975
12			980
13			985
14			987.5
15			990
16			992.5
17			995
18			997.5
19			1000
20			1002
21			1004
22			1006
23			1008
24			1010.5
25			1013
26			1015.5
27			1018
28			1021
29			1025
30			1037.5
31			1050
32			1075
33			1100
34			1150
35			1200
36			1250
37			1300
38			1350
39			1400

<sup>a</sup>See Table 6.2 for the names and thermal properties of the materials.

<sup>b</sup>Dimensions are given in feet.

<sup>c</sup>Heat generation occurs in this region.

within the unit cell are such that several rooms on both sides of a corridor are included. The contents of the two finite slab regions are distributed uniformly throughout their respective regions.

To obtain temperatures throughout the Repository, temperature changes calculated for two or more unit cells are superimposed at the appropriate space and time positions. If two or more types of waste are considered, each waste can be assigned to a different cell, and each of these cells must be calculated.

The second superposition model is 2-D(RZ). It consists of a single waste package located in an effectively infinite horizontal extent of the stratigraphy considered in the other 2-D(RZ) models (refer to Fig. 4.1 and Table 4.1). This model is used for determining the effect of loading sequence on temperatures in the near vicinity of a waste package. A comparison of results obtained with the simultaneous loading scheme [3-D(XYZ) models] with results obtained with various sequence loadings provides correction factors to be used with the 3-D(XYZ) results. Such comparisons also provide guidance in selecting optimum loading schemes.

The superposition technique is strictly applicable only when temperature-independent properties are considered. However, less overall error is introduced by using temperature-dependent properties with the superposition model, and the net error is reasonably small. Temperature-dependent properties were used with the 3-D(XYZ) superposition model; however, to date they have not been used with the 2-D(RZ) superposition model.

### 4.3 Model for Studying High-Level-Mine Fringe Area Effects

The above or similar superposition models can be used to obtain temperatures in fringe areas such as the alpha mine, shafts, adjacent rooms, etc. However, the 2-D(RZ) model shown in Figs. 4.1 and 4.5 will provide much of the same information. Figures 4.1 and 4.5 differ in that the latter figure includes the alpha facility, which is simulated by an annular void surrounding the disk source. This is a conservative approach to considering the insulating effect of the alpha mine on the high-level facility once the alpha mine is filled with waste and back-filled with crushed salt.

## 5. CRITERIA RELATED TO THERMAL ANALYSIS

### 5.1 Waste Temperatures

The maximum permissible temperature of the solidified waste is specified as the maximum temperature that existed during the solidification process. It appears that this temperature will range between 1100 and 2000°F, the specific value depending upon the process used.

### 5.2 Salt Temperatures

Permissible temperatures in the salt and other formations have thus far been derived from analyses of the room closure rate and the deformations in the shale bed above the mined area. An iterative procedure is required in which the thermal calculations are followed by a rock mechanics analysis, which, in turn, provides feedback for a new

thermal analysis. The most recent rock mechanics analysis indicates that the following interim thermal criteria should be used in the thermal parametric studies.

Consider a unit cell of the burial zone similar to those shown in Figs. 4.2 - 4.4, extending in the vertical direction from end to end of the waste container. The following conditions are specified: (1) no more than 1% of the salt in this unit cell shall be at a temperature above 482°F, and (2) no more than 25% of the salt in this unit cell shall be at a temperature above 392°F.

It is possible that more restrictive salt-temperature criteria will be specified in connection with brine migration and the effects thereof (production of radiolytic and chemical species such as H<sub>2</sub> and HCl). However, at this time, it does not appear that this will be the case.

### 5.3 Temperature Increases in Freshwater Aquifers, in Mineral Deposits, and at the Earth's Surface

The maximum permissible temperature rises in stagnant aquifers at depths of 100 and 300 ft are 15 and 50°F, respectively. Because of the low heat flux at and above these elevations, a small flow rate in the aquifers would reduce the temperature rise by a large factor.

Temperature rises anywhere in the geologic formations outside the AEC-controlled buffer zone shall be less than 1°F. This limiting value also applies to the earth's surface directly above the Repository.

## 6. THERMAL PROPERTIES

The thermal property data used in the most recent studies are essentially the same as the most up-to-date values discussed and listed in ref. 2. For the 3-D(XYZ) calculations, it was assumed that the shale was isotropic; however, thermal conductivity anisotropy was included for shale in the 2-D(RZ) calculations. The ratio of horizontal-to-vertical thermal conductivity for shale was assumed to be 1.5 on the basis of experimental data from the Lyons site.<sup>9</sup> The ratio presumably is temperature dependent, decreasing with increasing temperature. From the standpoint of calculating temperature rises quite some distance out from the edge of the Repository, it is conservative to use the maximum value of anisotropy for all temperatures; this was done in the 2-D(RZ) calculations.

The temperature dependence of the thermal conductivity of salt was considered in the 3-D(XYZ) calculations. For regions containing salt and shale it was assumed that the two materials were in discrete horizontal layers, and that most of the heat transfer in these regions occurred in a vertical direction. The effective thermal conductivity for the salt-shale regions was calculated from

$$k(T) = \frac{k_1(T) k_2}{f_1 k_2 + f_2 k_1(T)},$$

where

$k(T)$  = effective thermal conductivity for temperature  $T$ ,

$k_1(T)$  = thermal conductivity for salt at temperature  $T$ ,

$k_2$  = thermal conductivity for shale (measured in vertical direction),

$f_1$  = volume fraction of salt, and

$f_2$  = volume fraction of shale.

Calculated values of  $k(T)$  for the two salt-shale mixtures considered in the 3-D(XYZ) calculations are shown in Table 6.1. Other thermal properties used in the 2-D(RZ) and 3-D(XYZ) calculations discussed in this report are presented in Table 6.2.

Recent experimental results<sup>10</sup> indicate that the thermal conductivity of crushed salt is about twice the value that was used in the parametric studies. However, an uncertainty factor of 2 is not unreasonable for these studies, considering the possible variations in the nature of the actual backfill in a room.

## 7. RESULTS OF ANALYSES

### 7.1 Parametric Analysis of the High-Level Mine

The bulk of the results from the parametric analysis is presented in terms of the quantity (weight) of high-level waste nuclides (fission product and actinide nuclides) that can be accommodated per gross acre (room and pillar area), per net acre (room area only), and per waste package without exceeding permissible salt and waste temperatures, which, as will be shown later, are more restrictive than the other limiting conditions. The independent variables are: age of the waste, size of the room, and distance between the waste packages parallel to the length of the room. The recorded weights of nuclides include all waste nuclides including xenon and krypton, even though these and other gases will be collected separately during the solidification process. Thermal contributions from the gases are negligible.

Table 6.1. Thermal Conductivities of Salt and Salt-Shale Mixtures  
as a Function of Temperature [ $\text{Btu hr}^{-1} \text{ft}^{-1} (\text{°F})^{-1}$ ]

Temp. (°F)	Conductivity			Room and Pillar
	Salt	Salt (80%)– Shale (20%)	Salt (50%)– Shale (50%)	
32	3.53	2.29	1.50	1.83
122	2.90	2.06	1.43	1.515
212	2.43	1.85	1.37	1.28
302	2.08	1.68	1.31	1.105
392	1.80	1.53	1.25	0.965
482	1.60	1.41	1.19	0.865
572	1.44	1.31	1.15	0.785
662	1.33	1.23	1.11	0.730
752	1.20	1.14	1.06	0.665

Table 6.2. Summary of Thermal Properties — Most Recent Values

Material	Temp. (°F)	Thermal Conductivity [Btu hr <sup>-1</sup> ft <sup>-1</sup> (°F) <sup>-1</sup> ]			Density (lb/ft <sup>3</sup> )	Specific Heat [Btu lb <sup>-1</sup> (°F) <sup>-1</sup> ]
		Isotropic	Anisotropic			
			Vertical	Horizontal		
<u>Two-Dimensional (RZ) Model</u>						
1. Surface deposits	70	1.59	1.59	1.59	150	0.2
2. Shale	70	0.952	0.952	1.43	150	0.2
3. Shale and salt	70	2.78	2.78	3.12	140	0.2
4. Salt	300	2.06	2.06	2.06	135	0.22
<u>Three-Dimensional Models</u>						
5. Salt		<i>a</i>			135	0.22
6. Salt (80%)—Shale (20%)		<i>a</i>			138	0.216
7. Salt (50%)—Shale (50%)		<i>a</i>			142.5	0.21
8. Crushed salt	70	0.13			98	0.21
9. Calcine waste		0.25			113	0.22
10. Shale	70	0.952			150	0.2
11. Room and pillar		<i>a</i>			116.5	0.215

<sup>a</sup> See Table 6.1 for thermal conductivity as a function of temperature.

The following results do not specifically take into account the effects of mine loading sequence. It will be shown in Sect. 7.9 that this omission is valid for sequences being considered for the Repository.

#### 7.1.1 Permissible Loadings Based on Salt and Waste Criteria

Figure 7.1 shows the relative effects of the three limiting temperatures (waste, "1% salt," and "25% salt") for a typical case. As indicated, based on the 25% salt criterion, the surface density is nearly independent of pitch; based on the 1% criterion, it decreases somewhat with increasing pitch; and, based on the waste criterion, it decreases substantially with increasing pitch. These relative trends are valid for all of the cases considered in the parametric studies.

The minimum envelope of the three curves in Fig. 7.1 represents the maximum permissible loading. It is noticed that the peak waste temperature can be very restrictive for the larger pitches (heavier loadings per container). This situation can be improved substantially by using a solidified waste having a higher thermal conductivity and/or a higher permissible temperature. For example, one of the proposed wastes (pot calcine) has a 50% higher maximum permissible temperature (1650 vs 1100°F), but about the same thermal conductivity,<sup>11</sup> as was used in the parametric studies. For the particular case illustrated in Fig. 7.1, the higher permissible temperature barely eliminates the waste as a limiting factor for a 50-ft pitch.

Comparisons of results obtained for the 15-, 30-, and 50-ft rooms are shown in Figs. 7.2, 7.3, and 7.4 for 1-, 4-, and 10-year-old waste, respectively. Only the minimum envelope for the 1% and 25% curves and the portion of the waste curve below this envelope are shown in these

ORNL-DWG 72-6999

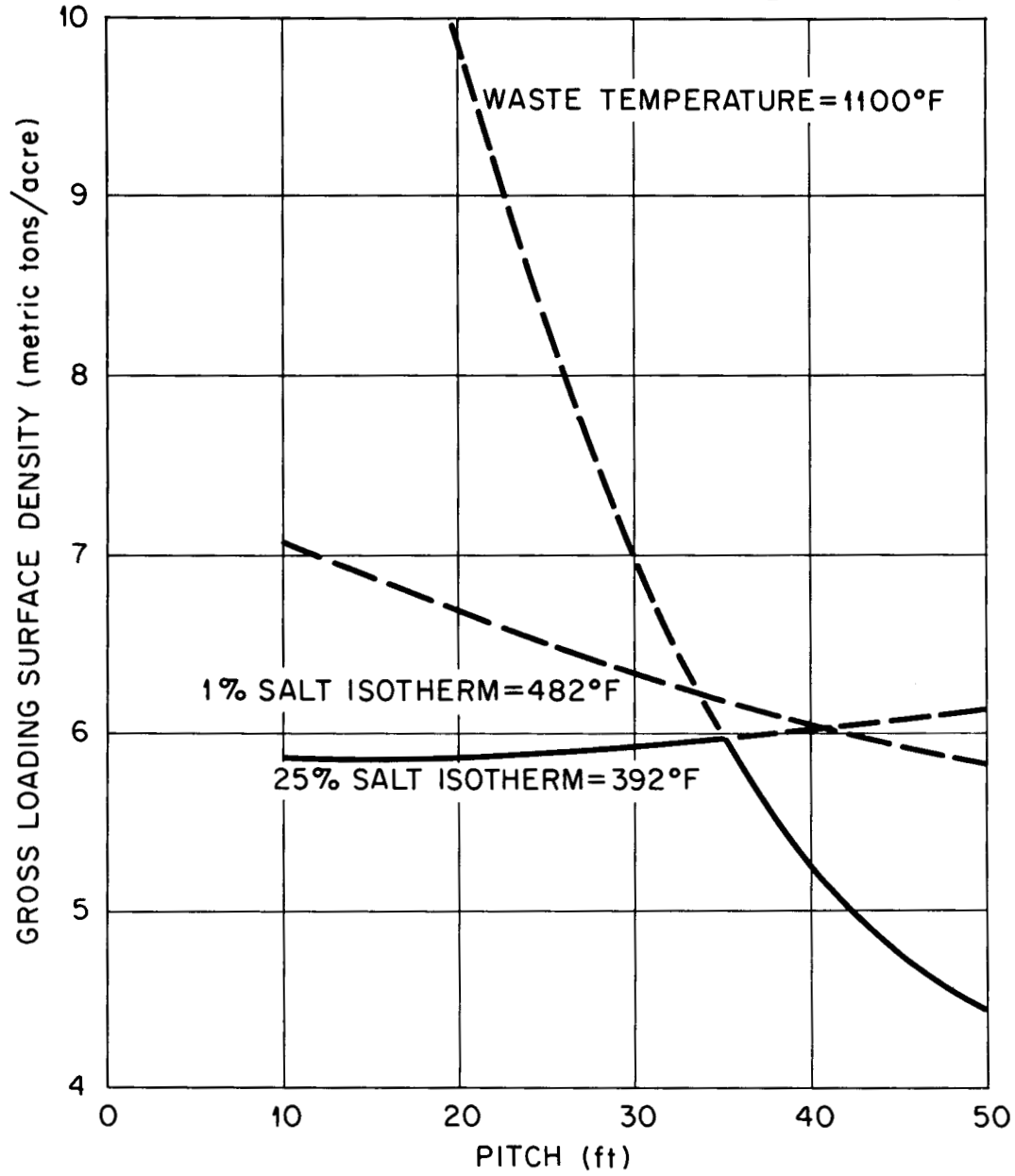


Fig. 7.1. Gross Loading Surface Density for 10-year-old Waste in a 15-ft Room in the High-Level Repository.

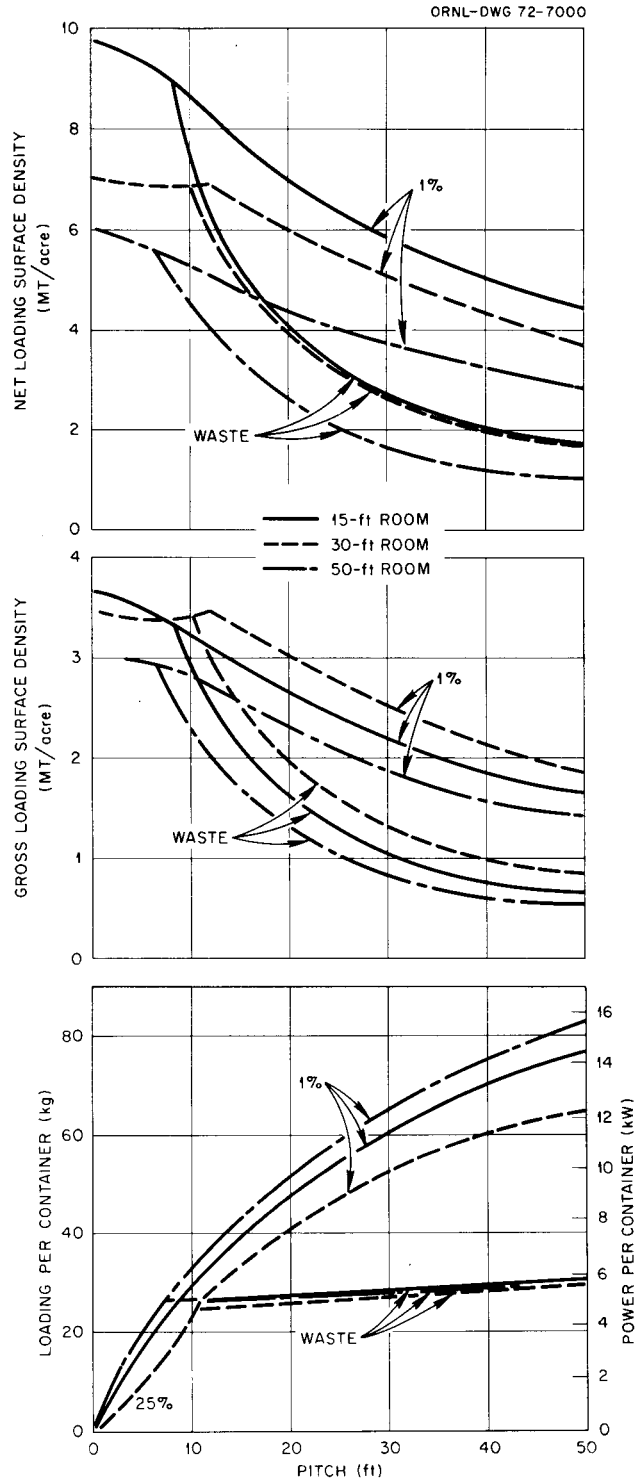


Fig. 7.2. Comparison of High-Level Repository Loading Surface Densities and Loadings per Waste Package for 1-year-old Waste and 15-, 30-, and 50-ft Rooms.

ORNL-DWG 72-7001

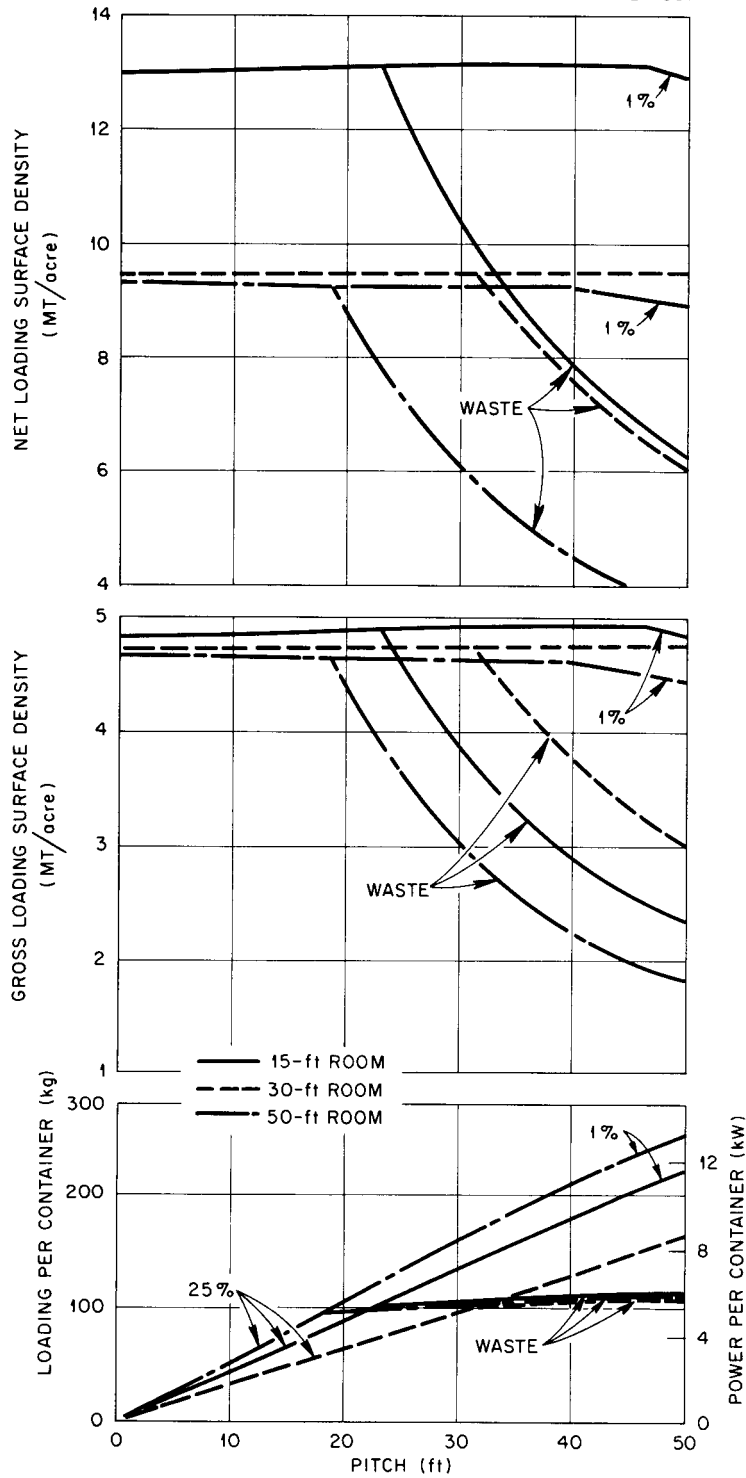


Fig. 7.3. Comparison of High-Level Repository Loading Surface Densities and Loadings per Waste Package for 4-year-old Waste and 15-, 30-, and 50-ft Rooms.

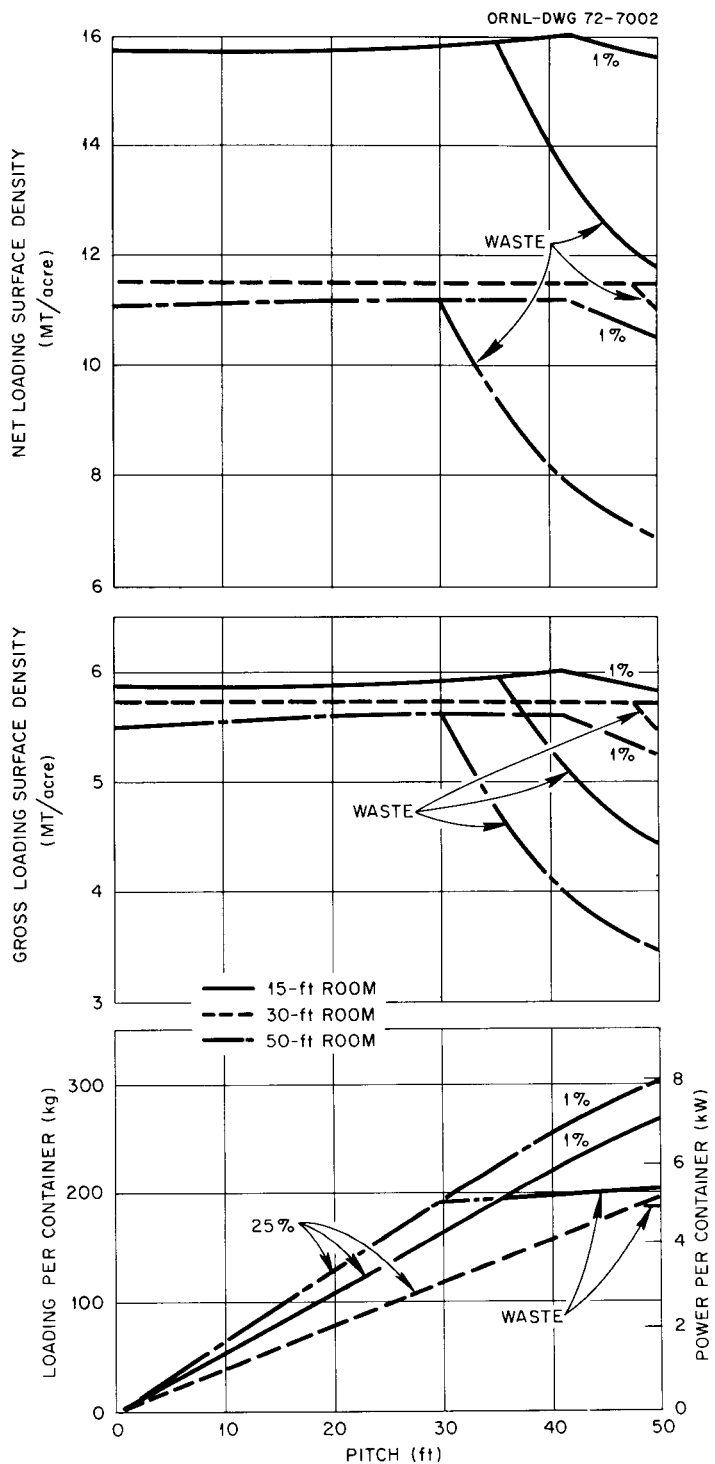


Fig. 7.4. Comparison of High-Level Repository Loading Surface Densities and Loadings per Waste Package for 10-year-old Waste and 15-, 30-, and 50-ft Rooms.

figures. Significant trends that can be observed in the figures are as follows:

1. The younger the waste, the smaller the pitch for which the 1% salt and the waste criteria become limiting.
2. For a particular waste age, the difference between maximum permissible gross surface densities for the three room sizes is small. However, there are significant differences between net surface densities. For instance, in the case of a 10-year-old waste (Fig. 7.4), the maximum permissible net surface density for a 15-ft room is about 37% greater than that for the other two room sizes. This constitutes a substantial saving in mining and salt disposal costs for the 15-ft room.
3. Increasing the pitch permits more waste per package, except where limited by the waste temperature.

Some of the data in Figs. 7.2 – 7.4 and similar data for 20-year-old waste have been cross-plotted in Fig. 7.5 for the 15-ft room to more clearly depict the effect of waste age. This figure shows the limiting gross loading surface densities based on the salt criteria.

Costs associated with the burial of the waste (i.e., Repository charges) are a function of the reciprocal of the curve in Fig. 7.5. Other costs that make up the total for high-level waste management are those for interim storage of the waste (as liquid and/or solid) aboveground, for solidification, and for transportation from the processing site to the Repository. Previous analyses<sup>3,4</sup> indicate that the summation of these costs as a function of waste age at burial will have a minimum somewhere between 3 and 10 years, likely closer to 10 years because of recent

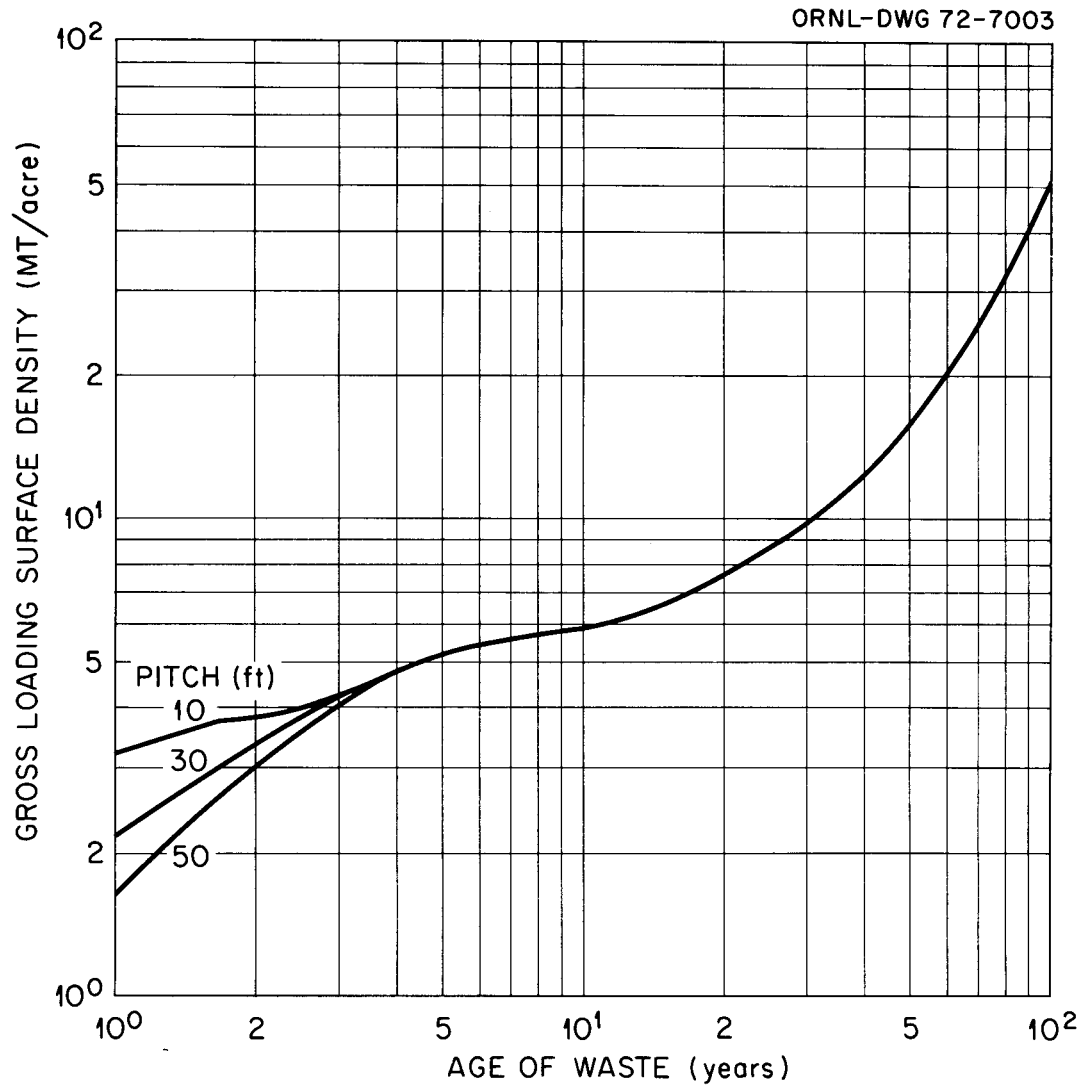


Fig. 7.5. Maximum Permissible Gross Loading Surface Density for a 15-ft Room vs Age of Waste (Based on Salt Temperature Criteria).

probable increases in estimated costs for the Repository.

It was possible to extrapolate the curve in Fig. 7.5 from 20 to 100 years because the effective half-life of the waste is nearly constant ( $T_{1/2} \approx 30$  years) from 20 to about 150 years, and the limiting salt temperatures peak within 40 years. A constant half-life results in a constant maximum permissible initial power level per waste package. This is shown in Fig. 7.6 for a 10-ft pitch. Thus, the shape of the loading curve from 20 to 100 years, as shown in Fig. 7.5, is the same as that of the quantity-of-waste-nuclides-per-unit-of-power curve shown in Fig. 7.7 (data also presented in Table 7.1).

#### 7.1.2 Temperature of the Waste Container Surface

Specific criteria do not as yet exist for the container surface temperature after burial. However, it is of interest to note the calculated peak temperature rises and the times at which they occur. This information is presented in Table 7.2 for the case in which the backfill around the waste package is assumed to have thermal properties similar to those of solid salt, and the container loading is limited by the salt temperature criteria. The container diameter is 6 in.; and the room size, pitch, and waste age are variables. It is observed that, for the range of variables considered in the parametric analysis, the peak temperature rises range from about 360 to 1840°F. The higher peaks are associated with the younger waste and larger pitches, for which higher power levels per container are permissible. The times at which the temperatures peak range from a fraction of a year for the higher temperatures to 30 years for the lower temperatures.

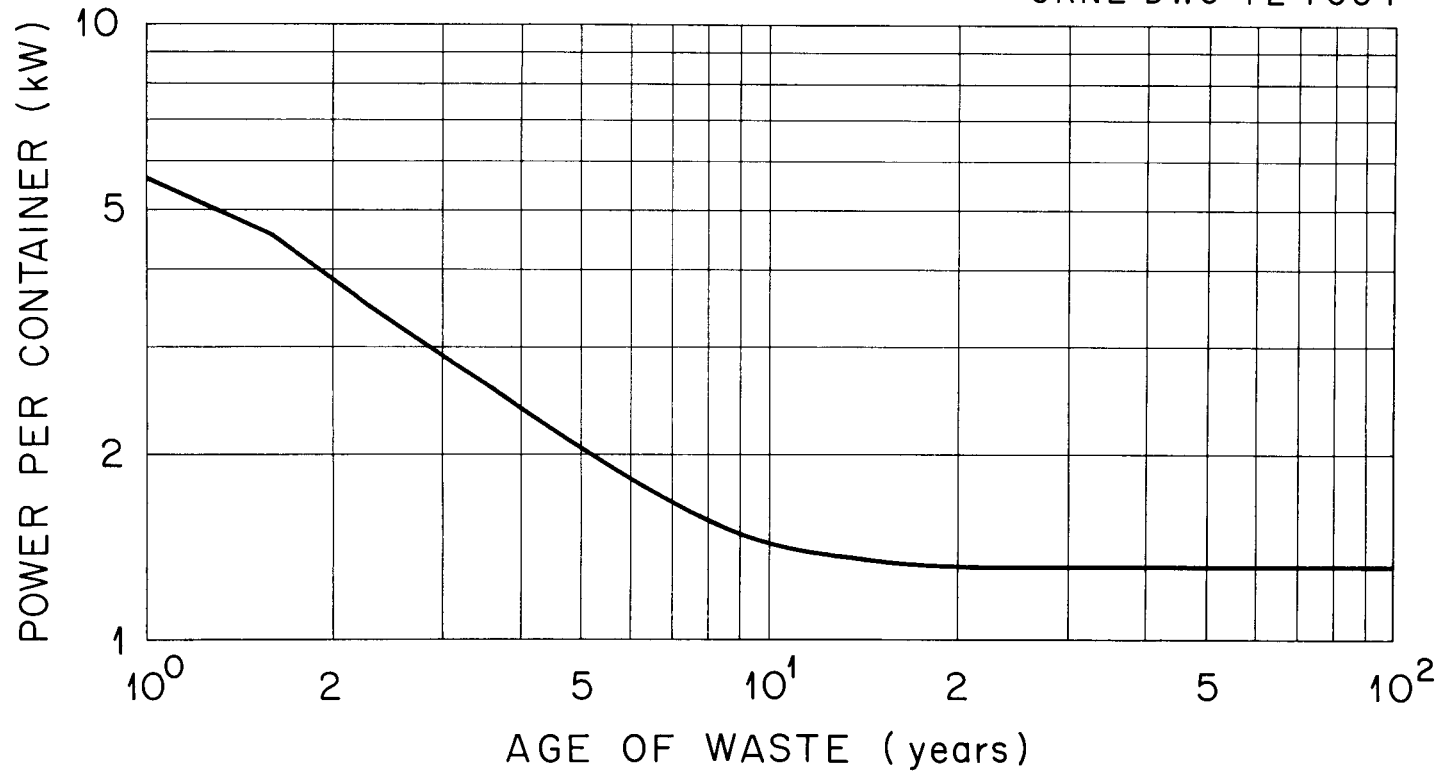


Fig. 7.6. Maximum Permissible Power per Waste Package, Based on Salt Temperature Criteria, vs Age of Waste for a 15-ft Room and 10-ft Pitch.

ORNL-DWG 72-7005

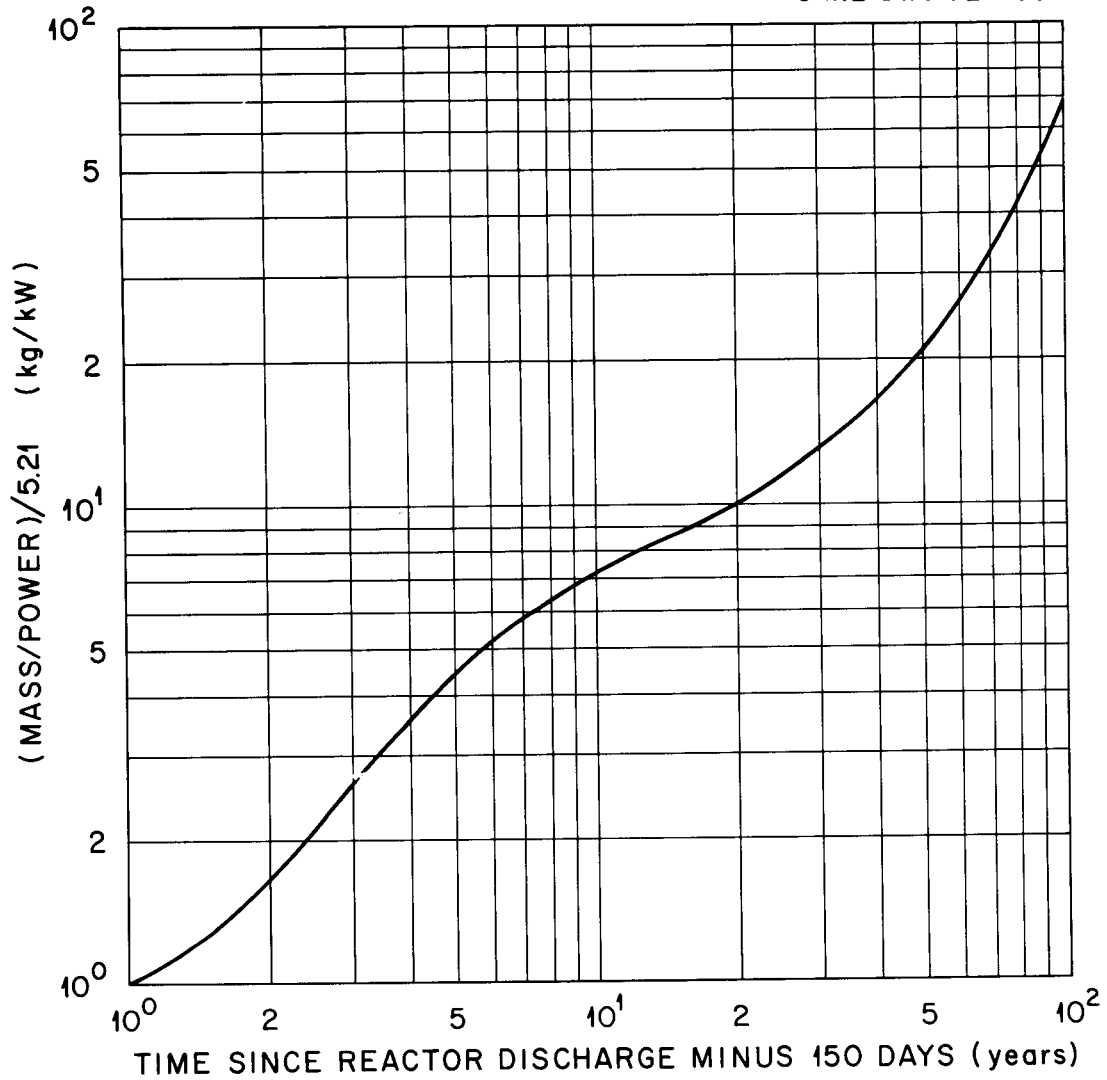


Fig. 7.7. Mass of Waste Nuclides per Unit of Waste Thermal Power vs Time Since Reprocessing at 150 Days Following Discharge from Reactor (Typical Waste from LWR).

Table 7.1. Mass of Waste Nuclides per Unit of Waste Thermal Power versus Time After Reprocessing<sup>a</sup>

Time After Reprocessing (years)	Mass/Power (kg/kW)
1	5.21
2	8.97
3	13.6
4	18.5
5	23.1
7	30.4
10	37.7
11	39.6
12	41.3
15	45.9
17	48.6
20	52.8
25	60.0
30	68.1
35	77.1
40	87.1
50	111
75	201
100	362

<sup>a</sup> Assuming that reprocessing takes place 150 days following the discharge of fuel from the reactor (typical waste from LWR).

Table 7.2. Maximum Surface Temperature Rises  
for 6-in.-Diam Waste Containers

Waste Age (years)	Room Width (ft)	Pitch (ft)	Peak Temp. Rise (°F)	Peak Time (years)	Thermal Power per Package (kW)
1	15	10	640	1/2	5.6 (1%)
		30	1220	1/4	11.4 (1%)
		50	1590	<1/8	14.4 (1%)
	30	10	550	3/4	4.5 (25%)
		30	1070	1/4	9.9 (1%)
		50	1370	1/8	12.1 (1%)
	50	10	690	3/8	6.1 (1%)
		30	1400	1/8	12.3 (1%)
		50	1840	<1/8	15.6 (1%)
4	15	10	370	30	2.4 (25%)
		30	700	1/2	7.2 (25%)
		50	1320	1/4	11.8 (1%)
	30	10	350	30	1.7 (25%)
		30	490	2	5.2 (25%)
		50	960	1/2	8.7 (25%)
	50	10	400	20	2.8 (25%)
		30	920	1/2	8.4 (25%)
		50	1640	1/4	13.6 (1%)
10	15	10	370	30	1.4 (25%)
		30	530	20	4.3 (25%)
		50	810	7	7.1 (1%)
	30	10	350	30	1.0 (25%)
		30	460	20	3.1 (25%)
		50	630	12	5.2 (25%)
	50	10	380	25	1.7 (25%)
		30	600	12	5.1 (25%)
		50	970	5	7.9 (1%)
20	15	10	360	30	1.3 (25%)
		30	520	20	4.0 (25%)
		50	800	<10	6.6 (1%)

### 7.1.3 Effect of Backfill Around Waste Container

Immediately following placement of a waste package in a hole, the annular space ( $\sim 2$  in.) between the container and the surface of the hole will be backfilled, probably with finely crushed salt. At  $212^{\circ}\text{F}$ , the thermal conductivity of crushed salt, prior to any reconsolidation, is about a factor of 10 less than that for solid salt.<sup>10</sup> Over a period of time, pressure and heat will cause the crushed salt to reconsolidate, and the thermal conductivity will presumably increase to the value for solid salt. The actual time behavior has not as yet been determined. In the parametric analysis, it was assumed that the peak temperatures in the waste and on the container surface occurred after the backfill reverted to solid salt. This permitted the use of thermal properties of solid salt for the backfill through the time-dependent calculation.

Two additional calculations were made in which a 2-in. annulus of crushed salt was placed around a 6-in.-diam package containing 4.3 kW of 10-year-old waste. Based on experimental results for finely crushed salt, the minimum thermal conductivity of the backfill was assumed to be  $0.2 \text{ Btu hr}^{-1} \text{ ft}^{-1} (\text{°F})^{-1}$ . The initial temperature of the container surface in one case was  $74^{\circ}\text{F}$ , the same as that for the surrounding formations; in the other, it was about  $700^{\circ}\text{F}$ , nearly the actual temperature to be expected at the time of burial. In each case the surface temperature after 1 day was  $800^{\circ}\text{F}$  and still increasing, assuming the backfill properties to be unchanged.

According to the Project Salt Vault experimental results,<sup>12</sup> reconsolidation of the backfill would terminate the temperature rise at about 1.5 days after burial, at a temperature less than  $830^{\circ}\text{F}$ , and the surface

temperature would have decreased to about 700°F by 100 days after burial. In the parametric analysis, which considered only solid salt, the peak surface temperature was about 600°F and occurred 20 years after burial. It is believed that the backfill will revert to solid salt long before a 20-year period has passed; thus it is likely that a minimum temperature will occur between 100 days and 20 years.

Since the initial peak occurs within only 1.5 days, the peak value will be independent of waste age, nuclide composition, and (to a large extent) room size and pitch. Thus, a single maximum permissible power level per package, based on the allowable waste temperature, can be specified for all waste ages and burial schemes considered in the parametric analysis. For a waste thermal conductivity of  $0.25 \text{ Btu hr}^{-1} \text{ ft}^{-1} (\text{°F})^{-1}$ , the temperature drops through the waste and across the backfill are about 109°F/kW and 140°F/kW, respectively, for the conditions stated above. The temperature rise at the surface of the hole at 1.5 days is about 53°F/kW. Consequently, the temperature rise at the center of the waste at 1.5 days is about 300°F/kW. For an allowable waste temperature rise of 1000°F, the maximum permissible power would be only 3.3 kW. If the allowable waste temperature rise were 1500°F, the permissible power would be 5 kW.

Increasing the diameter of the waste container will decrease the temperature drop across the backfill nearly proportionally. Suppose that the diameter is increased from 6 in. to 12 in. The heat flux will be decreased by a factor of 2, and the temperature drop will be 77°F/kW instead of 140°F/kW. There will also be a decrease in the hole surface temperature; however, this will be ignored at present. Thus, a conservative estimate for the waste temperature rise at 1.5 days for a 12-in.-diam

container would be  $109 + 77 + 53 = 240^{\circ}\text{F}/\text{kW}$ . If the allowable waste temperature rise is  $1100^{\circ}\text{F}$ , the permissible power is 4.6 kW. Consideration of the lower surface temperature for the hole increases the permissible power to about 5.0 kW.

A complete evaluation of the effect of the backfill material awaits compilation of more experimental data. In situ experiments are expected to be conducted in the near future.

#### 7.1.4 Power Limitations Imposed by Handling Operations Within the Repository

In the preceding discussion of results from the parametric analysis, limitations that will be imposed by factors at the Repository other than those directly associated with burial were not considered. It is not the intent of this report to analyze such factors in detail. However, it is of interest to briefly review them to see if they are significantly more or less restrictive than the others.

In the process of conveying a high-level waste package from a shipping cask to the mine-level transporter, the package must be cooled by thermal radiation to the walls of relatively large enclosures and by natural convection in air. All of the waste handling areas involved are to be cooled with circulating air and/or water to maintain adequately low air and enclosure temperatures for transient and steady-state conditions. Calculations<sup>13</sup> made for a 6-in.-diam waste package suspended vertically in air at  $70^{\circ}\text{F}$  and surrounded by walls at  $70^{\circ}\text{F}$  predict a container surface temperature of  $520^{\circ}\text{F}$  for a waste power of 0.65 kW/ft. The corresponding temperature drop across the waste, assuming the thermal conductivity of the waste to be  $0.25 \text{ Btu hr}^{-1} \text{ ft}^{-1} (\text{F})^{-1}$  is  $710^{\circ}\text{F}$ . For this case, the

centerline temperature of the waste is 1230°F. If the allowable waste temperature is 1100°F, the permissible power level would be 0.56 kW/ft or 5.6 kW in a 10-ft-long container. Although a maximum permissible waste container surface temperature has not as yet been specified, 520°F will not be limiting. Thus, from the standpoint of cooling in air, the power for a waste exhibiting the poorest expected thermal properties is limited to about 5 kW per package. Improved waste properties and/or a large-diameter container would result in a higher permissible value, based on the waste temperature, and also a higher surface temperature.

A thermal analysis<sup>14</sup> performed on the existing PSV mine-level waste-package transporter indicates that the maximum permissible power per package is about 5 kW, the limiting factor being the temperature of the waste. Shielding calculations<sup>15</sup> show that the power level for some waste ages is further restricted by the dose rate (including a contribution from neutrons) outside the transporter shielding. These limitations are illustrated graphically in Fig. 7.8, which is a plot of dose rate vs power for different waste ages, and Fig. 7.9, which shows the limiting powers based on dose rate and heat removal. It is observed that, based on dose rate, the allowable power is only 3.3 kW for a 1-year-old waste but is in excess of 5 kW for ages greater than 3.2 years.

An interesting consequence of the above power limitations, including the one imposed immediately after burial by the crushed salt backfill, is that the container surface temperatures for all acceptable cases will not exceed approximately 550°F. However, if the waste thermal properties and the transporter design are improved, higher powers might be permitted. This would result in higher surface temperatures.

ORNL-DWG 71-160A

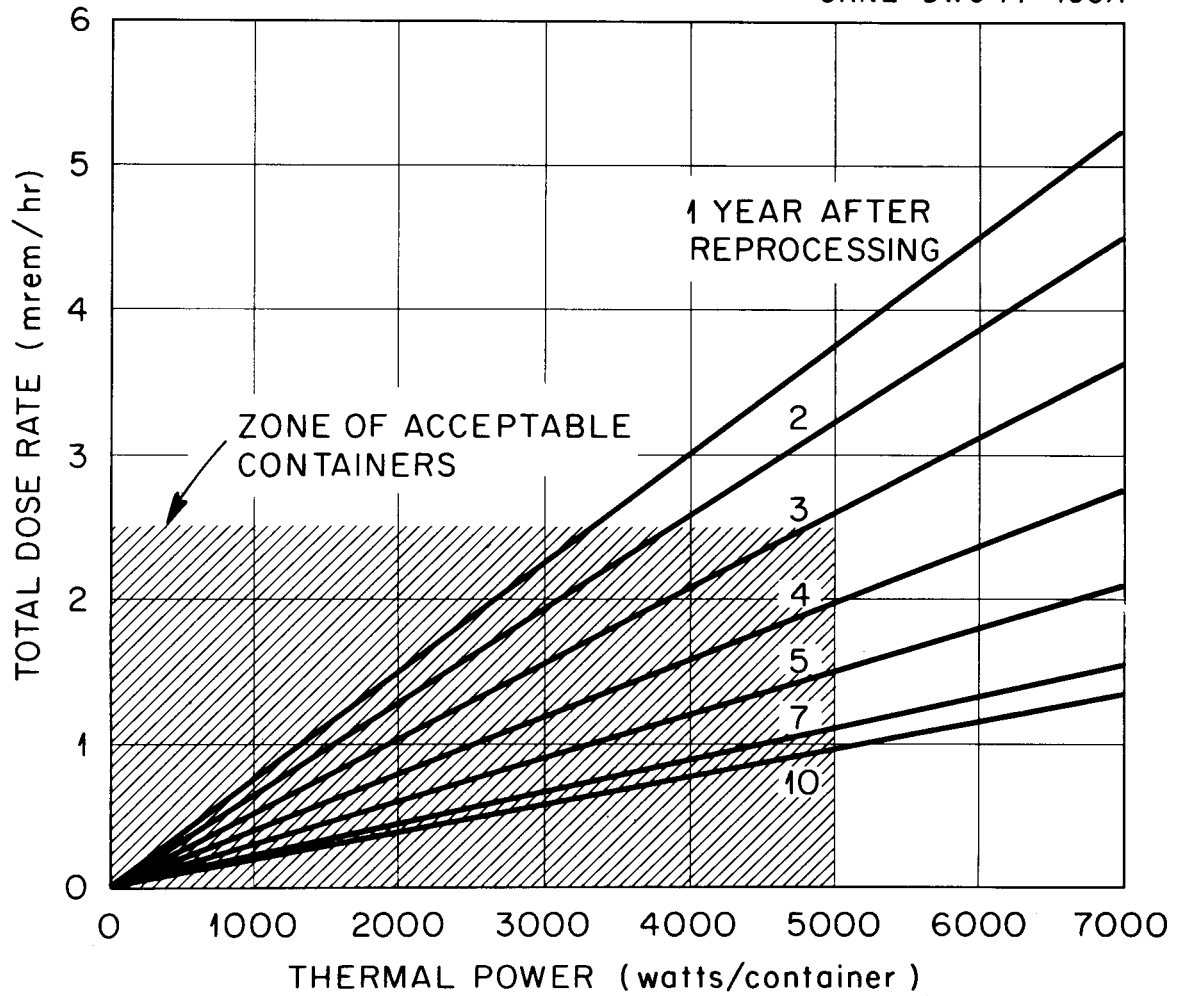


Fig. 7.8. Dose Rate at Surface of Existing Mine-Level Transporter vs Thermal Power and Age of High-Level Waste Within Transporter.

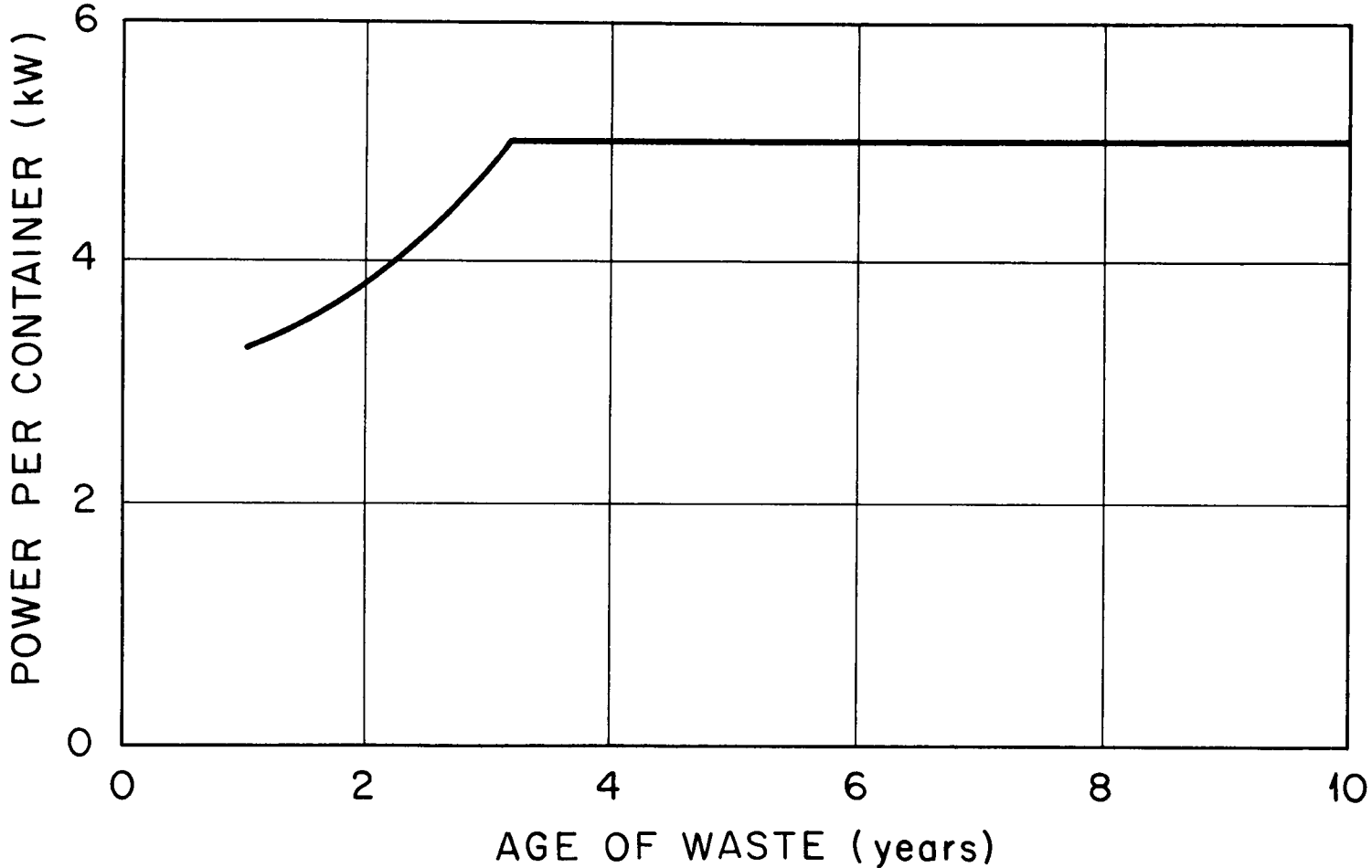


Fig. 7.9. Maximum Permissible Power per Waste Package, Based on Dose Rate and Thermal Limitations Imposed by the Mine-Level Transporter.

### 7.1.5 Multiple Rows of Waste Packages

As indicated by the results presented in Figs. 7.1 – 7.4, the optimum pitches for power levels below 1 or 2 kW are quite small. In some cases this can result in shielding and other operational problems during hole preparation and burial. The use of additional rows increases the pitch for the same loading surface density and hence might be a desirable feature for low loadings.

Multiple-row 3-D(XYZ) calculations were made with two and three rows in a 15-ft room and with three rows in a 30-ft room. The particular arrays are shown in Fig. 4.6. The pitches for the 30-ft room cases were 10 ft; 10- and 30-ft pitches were considered for the 15-ft room. An additional calculation was made for each of the two rooms with the waste homogenized over a 3-ft width for the 15-ft room and over a 22-ft width for the 30-ft room. The height of the homogenized zone was 10 ft. The age of the waste was 10 years in each case.

Results from the above calculations show that, for a specified room width, there is essentially no difference between permissible loading surface densities for all combinations of discrete packages considered. The permissible loadings were about 10% lower for the homogenized cases. For the cases involving discrete packages, the loading was limited by the 25% salt criterion. This same criterion was also used to evaluate the homogenized cases.

These results indicate a considerable amount of flexibility in accommodating low-power packages of all ages. The permissible loading surface densities will be equal to the values shown in Figs. 7.2, 7.3, and 7.4 for pitches less than 10 ft for 1-year-old waste, about 20 ft for 4-year-old waste, and 30 ft for 10-year-old waste.

### 7.1.6 Summary of Parametric Analysis

To summarize the results from the parametric analysis, it appears that there will be a cost advantage at the Repository in using 15-ft rooms and in delaying waste burial for about 10 years. This combination would permit as much as 6 metric tons of fission product nuclides (of the composition described herein) to be accommodated per gross acre (exclusive of corridors, etc.). If the thermal properties of the waste are about the same as those assumed in this particular analysis, and if the container diameter is at least 12 in., the maximum permissible loading per container will be 200 kg of waste nuclides. At the time of burial, this would be equivalent to a power level of 5.3 kW. The appropriate pitch for this case, using a single row of burial holes, is about 35 ft. A waste with better thermal properties would permit a greater loading.

## 7.2 Temperatures Throughout the Repository

Temperatures some distance from the mined area are independent of room size and waste package arrays; however, they are a function of the waste age and composition and, of course, the gross loading surface density. Results from the 3-D(XYZ) and 2-D(RZ) parametric analysis calculations indicate that the waste or local salt temperatures, rather than the temperatures farther out, are limiting over the waste age range of 1 to 20 years, considering the present set of criteria specified herein. Temperature-rise-vs-time curves obtained from a consistent set of 2-D(RZ) and 3-D(XYZ) calculations are shown in Fig. 7.10 for the case illustrated in Fig. 7.11. This latter figure shows a typical burial scheme, which, in three dimensions, corresponds to a 15-ft-room case with a 30-ft pitch.

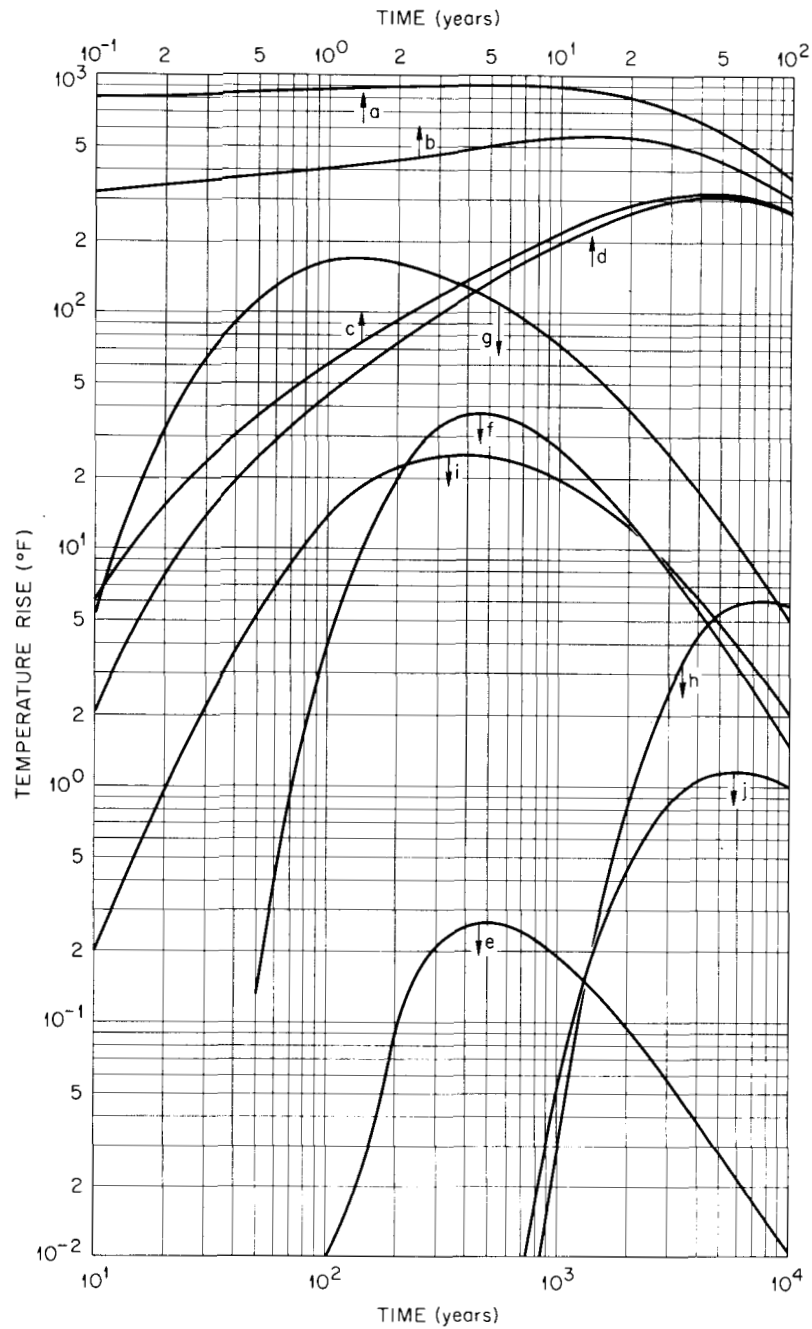
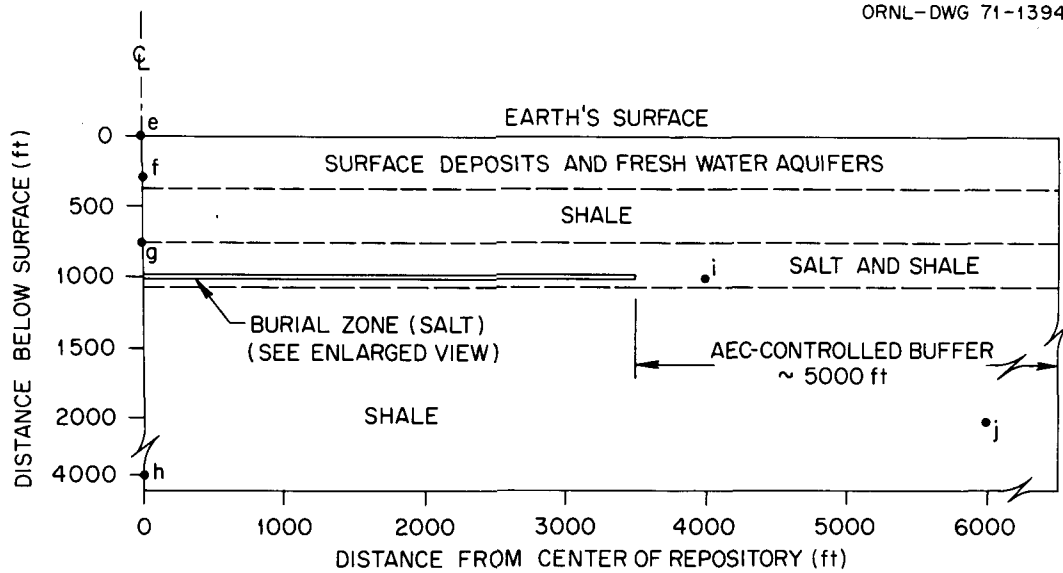
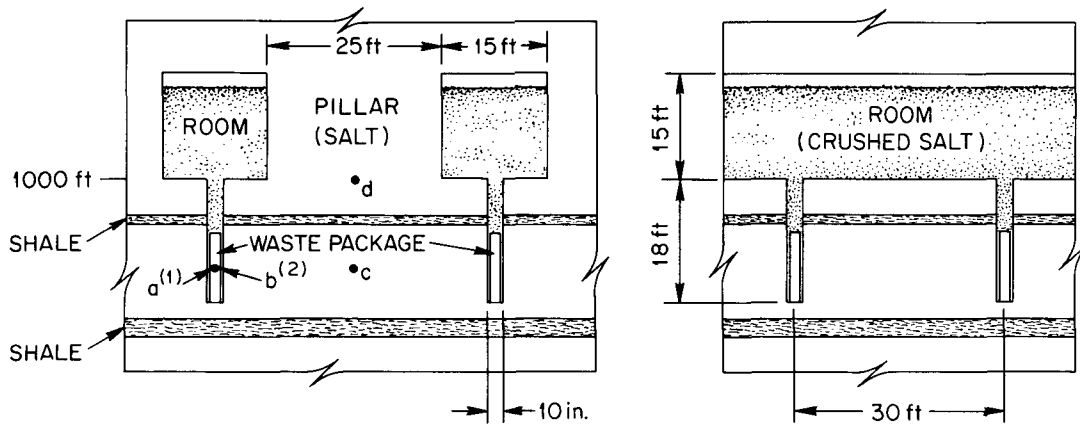


Fig. 7.10. Temperature Rise vs Time After Burial for 10-year-old LWR Calcined Waste, 15-ft Room, 25-ft Pillar, Single Row of 6-in.-diam Containers on 30-ft Pitch, Each Containing 165 kg of Waste Nuclides. (See Fig. 7.11 for identification of curves.)



VERTICAL CROSS SECTION OF REPOSITORY



1. a: CENTER LINE
2. b: SURFACE OF CONTAINER

END VIEW OF BURIAL ZONE FOR HIGH-LEVEL WASTE

SIDE VIEW OF BURIAL ZONE FOR HIGH-LEVEL WASTE

Fig. 7.11. Schematic Cross Section of Proposed High-Level Repository.

The gross loading surface density in the calculations was 6 metric tons per acre, and the waste age was 10 years. The specific locations for which temperature histories are recorded in Fig. 7.10 are identified alphabetically in Fig. 7.11.

Figure 7.10 shows that the waste centerline and the container surface temperature rises peak in about 5 and 15 years at 900 and 550°F, respectively. Near the base of the pillar, the maximum temperature rise is 300°F and the corresponding time 50 years. The maximum temperature rise at the base of the protective shale layer is 170°F (130 years), 37°F (500 years), in a stagnant freshwater aquifer at 300 ft below the surface, and 0.26°F (500 years) at the earth's surface. It is also observed that the permissible 1°F temperature rise in the geologic formations surrounding the Repository occurs at a location 2500 ft beyond the edge of the mined area (well within the AEC-controlled buffer zone) and about 2000 ft below the earth's surface. The corresponding time is 6000 years.

The 2-D(RZ) calculations indicate that when the maximum permissible loading surface densities are based on the 25% salt criterion, all peak temperatures and peak times for positions farther out are essentially independent of waste age. Thus, the peaks of curves c through j in Fig. 7.10 are also applicable for 3.7 metric tons of 1-year-old waste per gross acre (i.e., 700 kW/acre), 4.9 metric tons of 4-year-old waste per gross acre (i.e., 265 kW/acre) and 7.7 metric tons of 20-year-old waste per gross acre (i.e., 144 kW/acre). Prior to the peaks there are differences in the temperature curves. The younger the waste, the more rapidly the temperatures tend to increase.

Thermal conductivity anisotropy in the shale was not considered in the above 2-D(RZ) calculation. Including anisotropy tends to increase the temperatures at points beyond the edge of the mined area. When a horizontal-to-vertical thermal conductivity factor of 1.5 is used, the 1°F temperature-rise location occurs at 3000 ft beyond the edge rather than at 2500 ft beyond. The depth and the time are the same as for the isotropic case.

### 7.3 Repository Space Requirements

At the present time it is intended that the Repository will accept high-level waste through the year 2000. If nearly all of the waste is 10 years old at the time of burial, the amount of electrical energy generated that will provide waste for the Repository is, according to the most recent AEC prediction,  $2440 \times 10^6$  MWd. For the proposed 15-ft room and 25-ft pillar arrangement, the permissible gross loading surface density will be 6 metric tons of waste nuclides per acre. Waste generation calculations indicate that for a typical LWR there will be 40.5 kg of waste nuclides per metric ton of fuel, assuming the burnup to be 33,000 MWd per metric ton of fuel. Thus the burial area required per unit of thermal energy generated is 0.20 acre per  $10^6$  MWd; and the total area, exclusive of corridors, shafts, etc., is about 490 acres. It is estimated that the corridors and shafts will occupy about 10% of the area of the Repository. With this addition, the total area of the Repository excluding the AEC-controlled buffer area around the Repository would be 550 acres.

#### 7.4 Diameter of the Waste Container

The effect of the diameter of the waste container has been considered briefly. Increasing the diameter while holding the power constant decreases the heat flux at the container-salt interface. This tends to reduce local salt temperatures, the reduction becoming smaller as the distance from the interface increases. At radial distances corresponding to the peripheries of the 1% and 25% salt volumes, the reduction in temperature is negligible; however, it is significant at the container-salt interface. For example, increasing the container diameter from 6 in. to 14 in. decreases the interface temperature rise by about 17% for 10-year-old waste in a 15-ft room on a 50-ft pitch. In this case, the larger container would result in a 7% increase in the maximum permissible loading surface density. The effect is not as great for smaller pitches, but is somewhat greater for larger rooms ( $\sim 13\%$  for a 50-ft room and 50-ft pitch).

The actual diameter of a container specified for a particular waste will depend upon several factors, including the density of the solidified product. The specific volume of the solidified product is expected to be in the range 0.25 to 1 ft<sup>3</sup>/10<sup>4</sup> MWd.<sup>16</sup> For the case considered here, the burnup is 33,000 MWd/metric ton, and ORIGEN<sup>6</sup> results predict the waste nuclide production to be 40.5 kg/metric ton. Thus, the solidified waste-product "density"\* range is:

$$\frac{40.5 \text{ kg}}{\text{metric ton}} \times \frac{\text{metric ton}}{33,000 \text{ MWd}} \times \frac{10^4 \text{ MWd}}{(1 \text{ to } 0.25) \text{ ft}^3}$$

$$= 12.3 \text{ to } 49.1 \frac{\text{kg of waste nuclides}}{\text{ft}^3 \text{ of solidified product}}$$

---

\* This is not a true density since the 40.5 kg includes quantities of gases that will not actually exist in the solidified product, and the specific volumes do not include these quantities. However, the "density," as calculated, is consistent with the recorded weights and surface densities in this report and, when used with them, yields the correct solidified-waste volume.

Assuming the height of the waste in the container to be 10 ft, consistent with the height used in the parametric analysis described herein, the inside diameter of the container is computed from:

$$D = 0.357 \text{ ft}^{-\frac{1}{2}} \left(\frac{L}{\rho}\right)^{\frac{1}{2}},$$

where

D = inside diameter of the container,

$\rho$  = density of the solidified waste,

L = loading of waste nuclides.

Reference to Figs. 7.2 through 7.4 and consideration of heat removal and nuclear radiation limitations imposed during handling and transporting the wastes suggest that waste nuclide loadings per container will probably range from 25 to 300 kg. Corresponding container diameters are shown in Fig. 7.12 for the two "extreme" waste densities.

Consider a specific case in which the waste age is 10 years, the room size is 15 ft, and the waste thermal properties are the same as those used in the parametric analysis. According to Fig. 7.4, the maximum permissible loading of waste nuclides per container is 200 kg. If a solidified waste having the lowest anticipated density is used, the required container diameter would be 17.5 in. The existing high-level waste-package transporter accepts a container having a maximum diameter of 14 in. To comply with this limit a density of 26.9 kg/ft<sup>3</sup>, which corresponds to 0.46 ft<sup>3</sup>/10<sup>4</sup> Mwd, would be required.

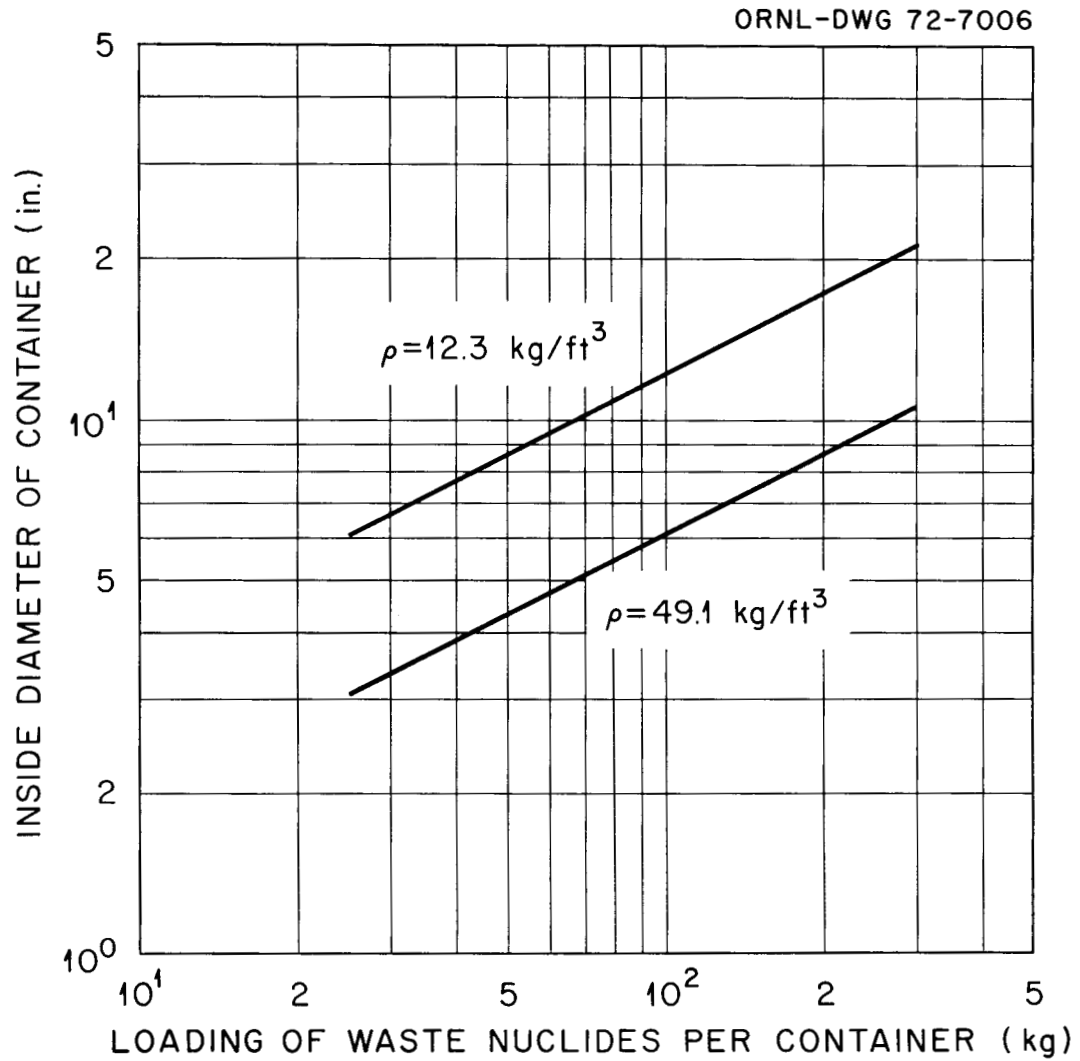


Fig. 7.12. Container Inside Diameter vs Waste Nuclide Loading for a Range of Waste Solidified Product Densities and for a Waste Height Within the Container of 10 ft.

### 7.5 Temperatures in the Fringe Areas

Working areas adjacent to loaded portions of the high-level mine must be maintained at sufficiently low temperatures to permit safe operation of the Repository. These fringe areas include the corridors, shafts, areas undergoing excavation and loading, and perhaps an adjacent alpha facility. Temperatures in these areas are a function of the mining and loading sequences, the distances between these areas and heat sources and the ventilation scheme. Nearly any practical loading sequence is such that mining and/or drilling and burial operations must take place adjacent to areas that have previously been loaded with waste. For a particular sequence and ventilation scheme, both of which tend to be established on the bases of other factors, the distances between the new and the old areas can be specified such that temperatures are not excessive. Of course, there is a desire to minimize these distances so as to minimize the total land area required for the Repository.

Temperatures in the fringe areas have been calculated with a 2-D(RZ) model (Fig. 4.5 and Table 4.5) and a 3-D(XYZ) superposition model (Fig. 4.7 and Table 4.6). The 2-D(RZ) model includes an annular void surrounding the high-level mine to simulate the worst possible insulating effect of the alpha mine during the early years. Also, the full size of the high-level mine is included, and all waste is assumed to be loaded simultaneously. These features tend to result in higher-than-actual temperatures for the fringe areas, but not substantially higher because of the time constants and times of interest involved. Homogenization of the source regions has the opposite effect for locations very close to the rooms. However, the heterogeneity effect is quite small at 50 or

more feet out from the source.

Figure 7.13 shows temperature-rise-vs-time curves for specific locations in the salt surrounding the source region. The results presented in this figure correspond to the "typical" LWR high-level, 10-year-old waste discussed previously and are conservatively applicable for younger wastes when the 25% salt criterion is limiting (refer to Sect. 7.1.1).

Results from the 3-D(XYZ) superposition model take into account the loading sequence effect, which tends to result in lower temperatures than those calculated with the 2-D(RZ) model. A comparison of results from the superposition and 2-D(RZ) calculations shows negligible differences for positions 50 ft or more away from the source.

Although limiting temperatures have not as yet been specified for the fringe areas, it is of interest to examine the temperatures at a few points using a tentative layout of the mine for the Lyons site (Fig. 7.14). Ten years after burial is commenced in the first section of the repository (years 1 - 10), burial must commence in an adjacent section (years 11 and 12). The width of the salt column (buffer) between the back ends of rooms in adjacent sections is tentatively specified as 50 ft. The temperature rise in the salt at the location of the back end of the new room just prior to excavation at 10 years would be about 45°F, which probably is not excessive for mining, drilling, and burial. As the burial rate accelerates, the delay time between sections is considerably less, and hence the temperature rises in new sections at the time of their operation are less. An exception to this general rule involves the main corridor, sections on the opposite side of the main corridor, and a final

ORNL-DWG 72-7007

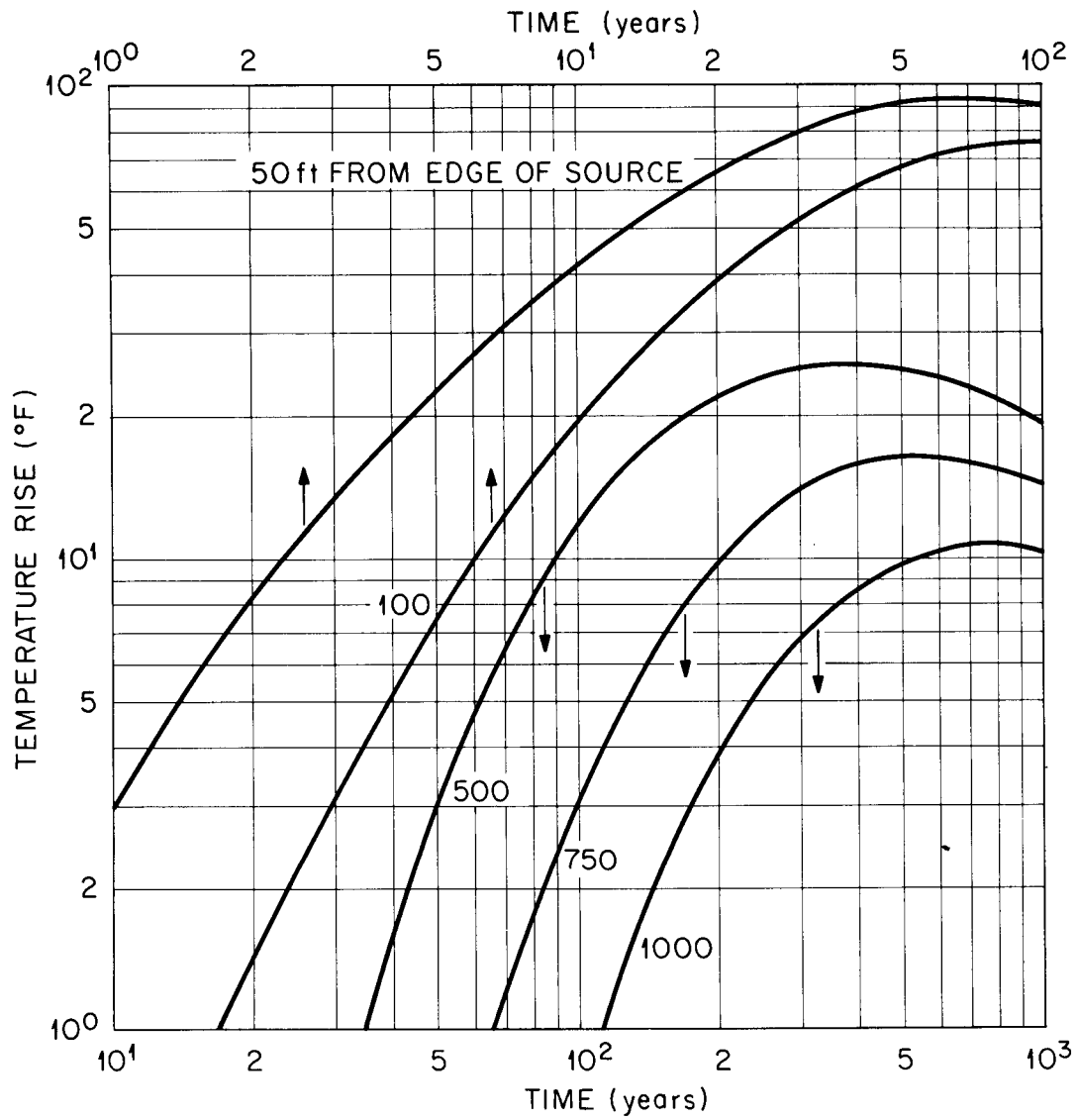


Fig. 7.13. Temperature Rise vs Time Since Burial for Locations Near Edge of Source Region: 158 kW/Acre of 10-year-old LWR Waste.

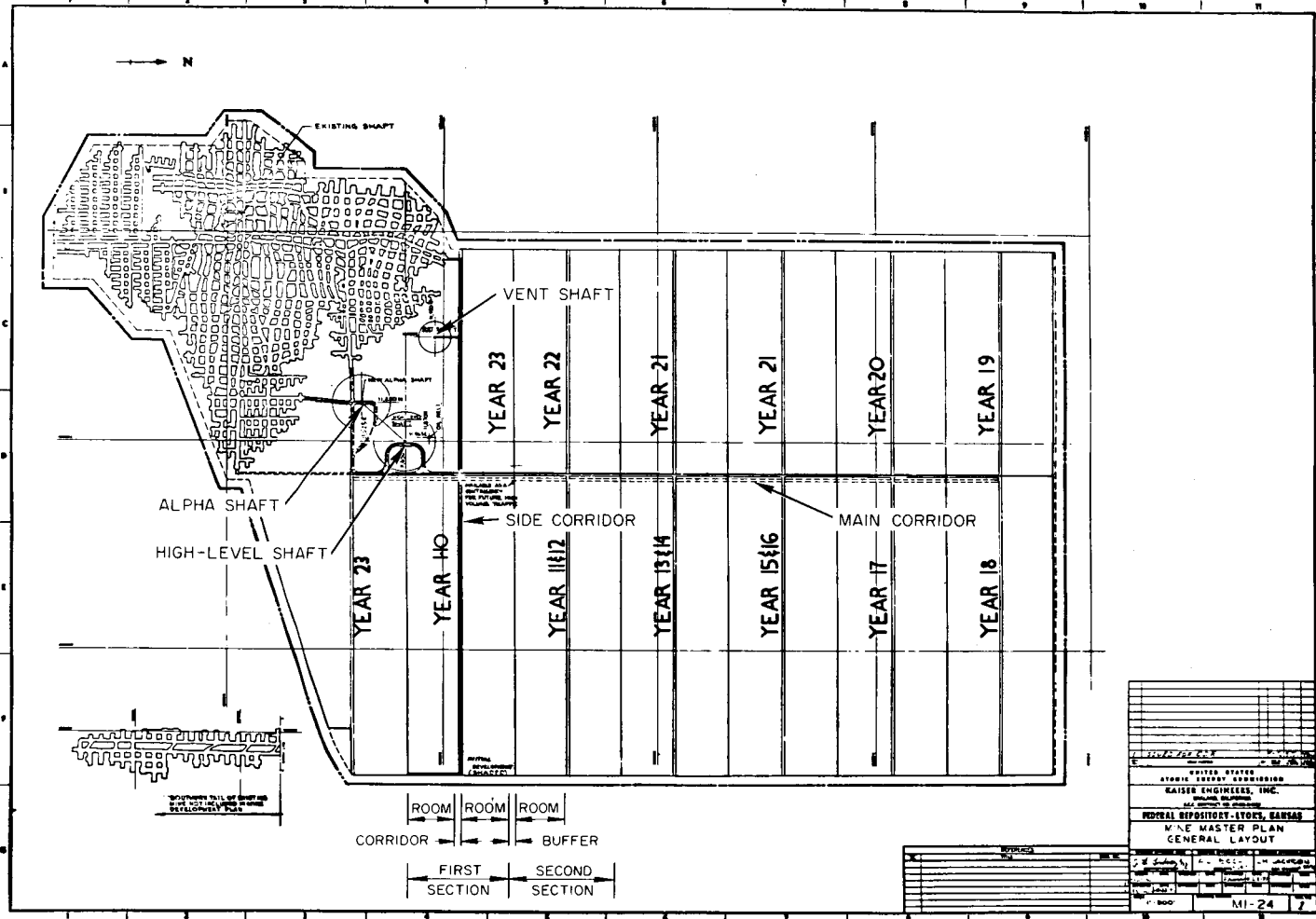


Fig. 7.14. A Proposed High-Level Mine Layout and Loading Sequence with an Adjacent Alpha Mine: Lyons Site.

section (year 23) that is adjacent to the first. A portion of the corridor that is used essentially up until mine decommissioning and a section receiving waste at about this same time are directly opposite the first section and thus are exposed to waste buried about 13 years beforehand. Suppose that, in the absence of surface cooling by means of the ventilating air, the maximum permissible surface temperature rise in the corridor is 50°F. Assuming that decommissioning takes place in 25 years, the closest permissible approach of waste in the first section to the main corridor just outside this section would be about 80 ft. The opposite section, which receives waste about 23 years after burial is initiated in the first section, is separated from the first section by the main corridor; therefore, the temperature rise at the entrance to the new section would be less than 50°F.

The last section to be filled with waste is adjacent to the first section and is separated by 50 ft of salt at the back ends of the rooms. At 23 years the temperature rise at the back end of a new room opposite one of the first rooms loaded would be about 75°F. If the distance between the two sections involved were 100 ft instead of 50 ft, the temperature rise would be only 40°F.

The high-level shaft is located about 500 ft from waste in the first section. Its temperature rise at the end of 25 years would be less than 1°F.

The proximity of the alpha waste to the high-level waste and a permissible temperature rise in the alpha waste due to the high-level waste have not been specified. However, at this time it appears that a 25°F rise, corresponding to a distance of 500 ft and a peak time of about

400 years, would be acceptable. Further discussion of temperatures in the alpha mine is included in Sect. 7.8.

### 7.6 Removal of Heat from Rooms with Ventilating Air

Several 2-D(XZ) calculations (see ref. 1 for model detail) were made for cases in which the interior of a room directly above buried waste was cooled with ventilation air. The coolant flow rate was such that the coolant film heat transfer coefficient ( $h_f$ ) was controlled almost entirely by natural convection. Calculations were made with  $h_f = 0.1, 0.4, 0.7,$  and  $1 \text{ Btu hr}^{-1} \text{ ft}^{-2} (\text{°F})^{-1}$ . It was assumed in any one calculation that the  $h_f$  value was uniform over all room surfaces. In actuality,  $h_f = f(\Delta T)$  (see Fig. 7.15), where  $\Delta T$  is the difference in temperature between the surface and the bulk coolant.<sup>17</sup> Furthermore,  $\Delta T$  is not uniform over the surfaces. However, the approximation of uniform  $h_f$  is adequate for obtaining preliminary information on the effect of air cooling.

Figure 7.16 shows a plot of the temperature rise at the center of the floor of a 15-ft room as a function of time for the four different values of  $h_f$  and for the case in which the room is partially filled with crushed salt and topped off with an insulated void. If it is assumed that sufficient air is circulated to maintain the room air temperature at about the original ambient ( $74\text{°F}$ ), then the temperature rises in Fig. 7.16 represent the temperature drops across the coolant film. Referring again to Fig. 7.15, it is observed that  $h_f$  for these temperature drops ranges between  $0.5$  and  $1 \text{ Btu hr}^{-1} \text{ ft}^{-2} (\text{°F})^{-1}$ . The actual temperature drop, estimated using the information in Figs. 7.15 and 7.16, is expected to be

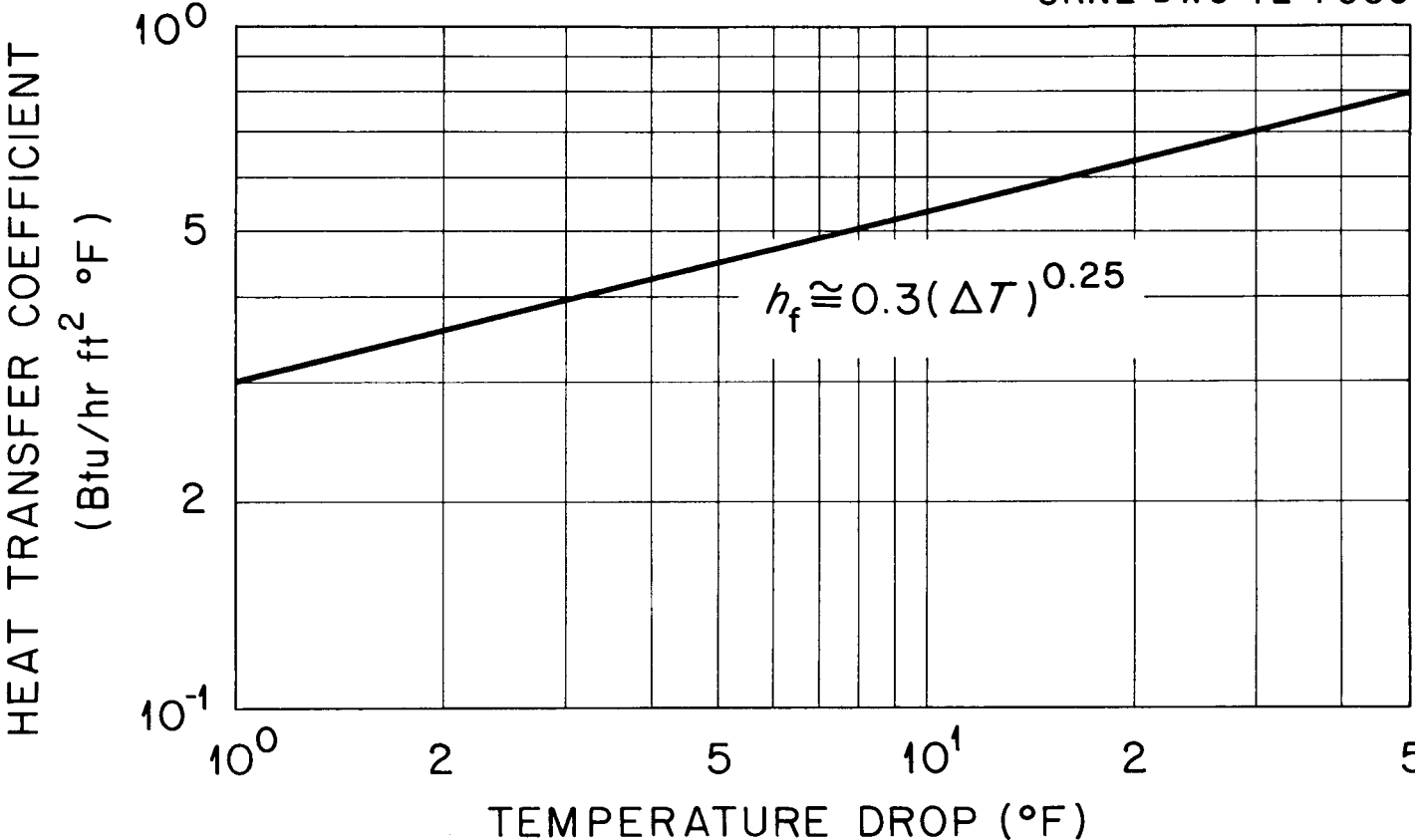


Fig. 7.15. Natural Convection Heat Transfer Coefficient for Air vs Temperature Drop Across Film.

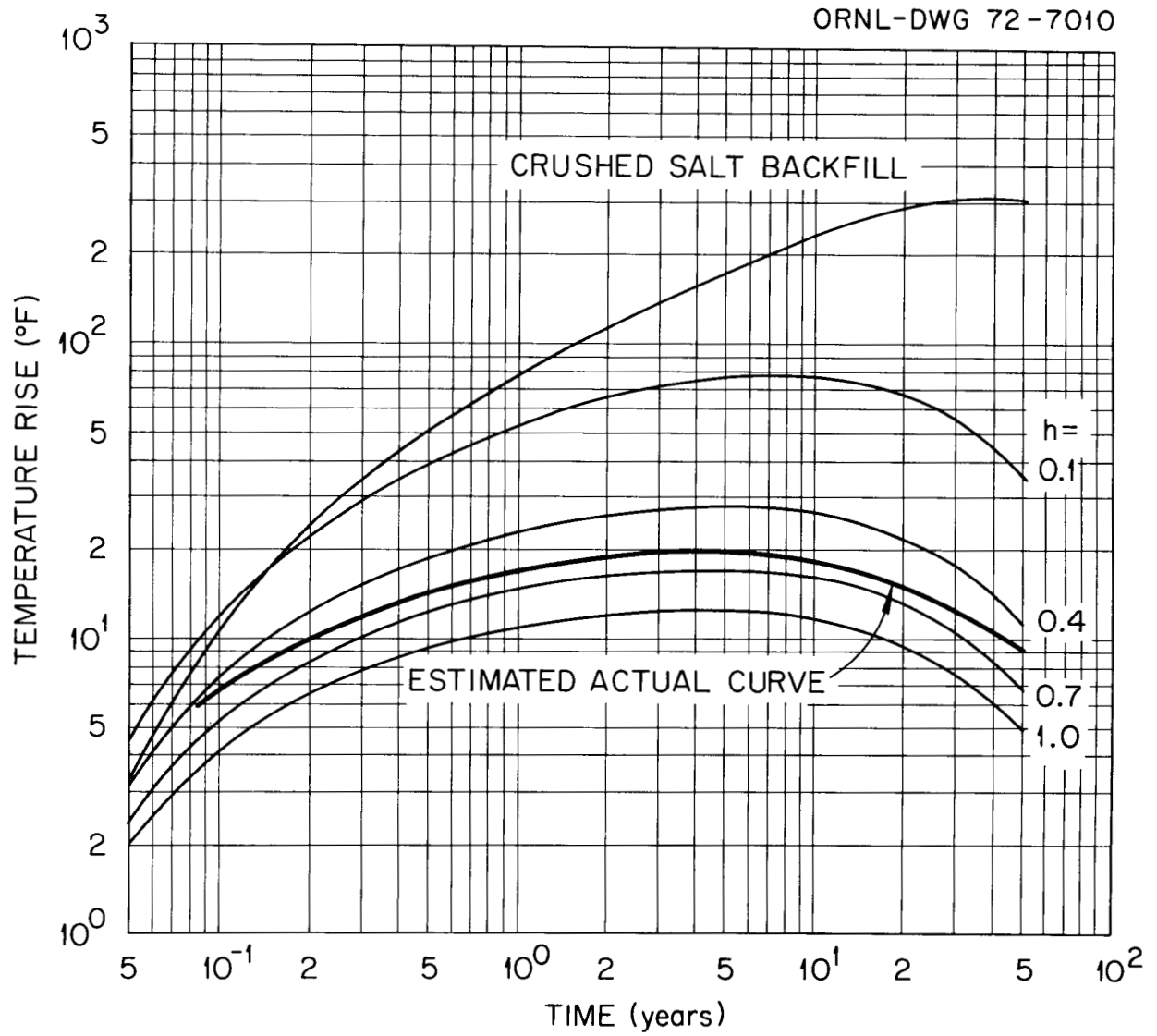


Fig. 7.16. Temperature Rise at Center of Floor vs Time for Different Heat Transfer Coefficients on Surfaces of Room: 10-year-old LWR Waste, 158 kW/Acre, 15-ft Room.

slightly above the  $h_f = 0.7$  curve in Fig. 7.16. This means that the maximum temperature rise in the floor with ventilating air passing through the room will be about 20°F.

The amount of heat removed from a 15-ft room with the ventilating air can be roughly estimated from

$$\frac{P}{L} = 1.3(\Delta T)^{1.25},$$

where

$P$  = power (W),

$L$  = length of room (ft),

$\Delta T$  = temperature drop across coolant film (°F).

This equation is plotted in Fig. 7.17, which shows that, for  $\Delta T = 20^\circ\text{F}$ ,  $\frac{P}{L} = 55$  W/ft. The power per unit of length of the room that corresponds to 158 kW/acre is  $\frac{P}{L} = 145$  W/ft. Thus, a maximum of about 40% of the waste heat can be removed with the room ventilating air, the maximum rate occurring at about 5 years after burial.

The specified flow rate of ventilating air in a room is 20,000 cfm. If 55 W/ft is being removed with this air, the temperature rise of the air would be about 5°F.

A primary implication to be drawn from the above results is that temperature rises in the fringe areas mentioned in Sect. 7.5 can be substantially reduced with ventilating air. This provides an additional degree of flexibility in working out a loading sequence pattern.

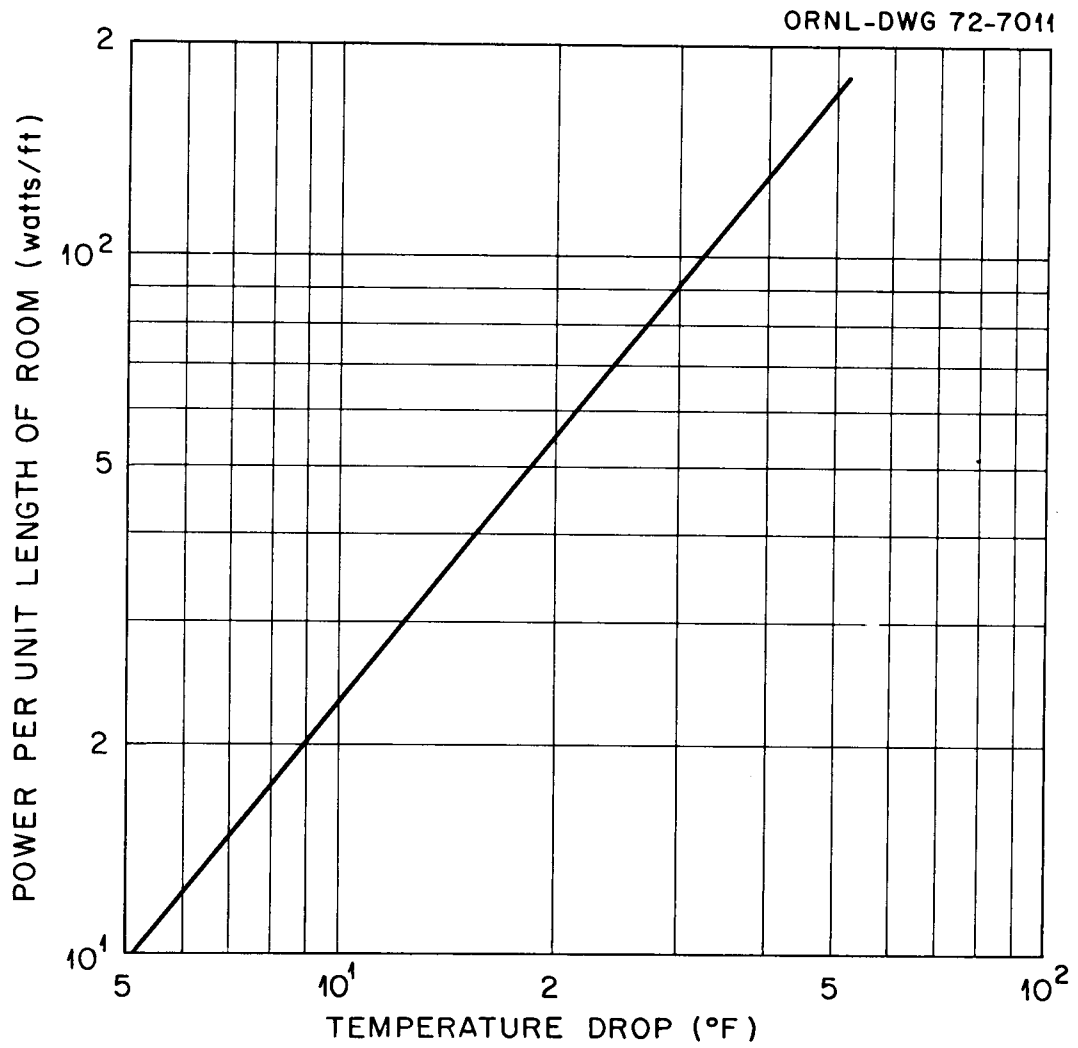


Fig. 7.17. Ventilating-Air Heat Removal Capability vs Temperature Drop Across Coolant Film.

### 7.7 Cladding Hulls

Calculations were made for cladding hulls that were buried 1 and 3 years after reprocessing. There is little change in the effective half-life over this period of time; thus the permissible power per waste package is essentially the same for the two ages. The 25% salt temperature criterion was limiting for a 15-ft room and a 10-ft pitch, the conditions for which the calculations were made. The maximum permissible power per package was 3.3 kW, or 359 kW/gross acre.

The expected power from 1-year-old cladding hulls is about 95 W per ton of fuel (U + Pu), and the compacted volume is 2.1 ft<sup>3</sup>/ton. It has been proposed<sup>18</sup> that a 10-ft-long, 9-in.-diam cylindrical container be used to contain the hulls for burial. Consequently, the initial power per package is 200 W for 1-year-old hulls, and 147 W for 3-year-old hulls. For two rows of waste packages in a 15-ft room, the pitches corresponding to these powers and to the maximum permissible power surface density are 1.2 ft and 0.9 ft, respectively.

According to ref. 18, shielding during burial operations will require about 3 ft between holes in the floor in the case of the 1-year-old hulls. Thus, burial in a 15-ft room will not be very efficient. The use of multiple rows in a larger room tends to rectify this situation. A 23-ft room with a 27-ft pillar, six rows of waste packages spaced 3 ft apart, and a pitch of 3 ft results in the limiting power surface density with 200 W per package. In ref. 18 it was estimated, on a somewhat different basis, that 15 rows in a 50-ft room with a 3-ft spacing and pitch would be acceptable. However, the power surface density for this arrangement would be 25% too high.

### 7.8 Temperatures in Combustible Alpha Waste

Temperatures in the alpha waste are equal to the summation of the alpha- and high-level-waste contributions to the temperature of the surrounding salt formation and of the temperature drop in the waste and backfill material in the burial rooms. In a previous analysis,<sup>2</sup> a one-dimensional model was used to determine temperatures in the formations above and below the central portion of the alpha burial horizon, independent of the high-level facility. The high-level contribution can be obtained from the 2-D(RZ) results discussed in Sect. 7.5 and can be superimposed on the 1-D(Z) results. This is somewhat conservative at the edge of the alpha facility because the 1-D(Z) model does not consider the radial degradation of the temperature in this area. Based on this conservative approach, the maximum temperature of the salt just above the alpha waste at the edge of the alpha facility nearest to the high-level facility (assuming a 500-ft separation) is about 140°F. The contribution from the high-level waste is 25°F.

With a compaction factor of 10, the peak average power density in the alpha waste is expected to be about 0.042 W/ft<sup>3</sup>. In the previous analysis, segregation within an individual container was ignored and the effective thermal conductivity for the waste and backfill material was assumed to be 0.1 Btu hr<sup>-1</sup> ft<sup>-1</sup> (°F)<sup>-1</sup>. This resulted in a temperature drop from the center of the "homogenized" waste to the solid salt of about 20°F. The peak power density actually occurred prior to the peak salt temperature so that the addition of the above temperatures (which yields 160°F) is somewhat conservative, based on the particular assumptions considered.

A continuing evaluation of the alpha facility indicates that a conservative lower limit for the thermal conductivity of the waste and backfill is  $0.02 \text{ Btu hr}^{-1} \text{ ft}^{-1} (\text{°F})^{-1}$ , which is approximately the value for stagnant air at the temperatures of interest. This increases the peak waste temperature drop to  $100\text{°F}$  and the waste temperature to  $240\text{°F}$ , if the source is assumed to be uniformly distributed. Segregation within an individual container can increase the drop considerably.

The maximum permissible uniform temperature for combustible alpha waste has been tentatively specified as  $350\text{°F}$ , based on experimental work<sup>19</sup> conducted at ORNL with typical combustible alpha wastes in 55-gal metal drums. This temperature is less than the "handbook" ignition temperatures for spontaneous combustion of all of the different types of anticipated wastes. It is recognized that segregation of the nuclear energy source within a container might result in local temperatures in excess of  $350\text{°F}$  and in excess of handbook values for spontaneous combustion ignition temperatures. However, at the present time, it is believed that the ignition temperature for compacted waste in a drum containing a limited amount of oxidant will be higher than the handbook value. It is also believed that ignition in one of these packages would not be objectionable because the lack of oxidant would limit combustion to a small fraction of the waste in a single container. Further studies regarding segregation and limiting temperatures are being conducted.

### 7.9 Sensitivity of Maximum Temperatures to Loading Sequence (Phasing)

The temperature change at any point in the Repository can be thought of as the sum of temperature-change contributions from each of the many waste packages. For the hypothetical case of temperature-independent properties, the conduction equation is linear and the temperature-change distributions for single sources can be superimposed in accordance with any desired space and timewise loading scheme to obtain the total temperature change at a given point. Typical temperature-rise distributions in space and time for a single waste package are shown in Fig. 7.18. At each point in space, the temperature curve exhibits a maximum; and, the farther the point from the source, the smaller the maximum value and the longer it takes to occur. Thus, for the case of multiple sources, the temperature at a particular point in space and time is dependent upon the relative positions and times of burial of all the sources. This can be described as a phasing effect.

To illustrate the phasing effect, consider a concentric-circle burial array with 40 ft between circles and about 40 ft between adjacent packages on any particular circle. (This closely resembles single-row burial of high-level waste in 15-ft rooms with a 40-ft pitch.) The problem is to find the maximum surface temperature of the central package for different loading sequences.

Each curve in Fig. 7.18 can be thought of as the contribution made by a single package, located the indicated distance away, to the central package. Suppose that all packages are loaded at the same time. For the circular array considered, the number of containers on circle  $n$  is  $2\pi n$ .

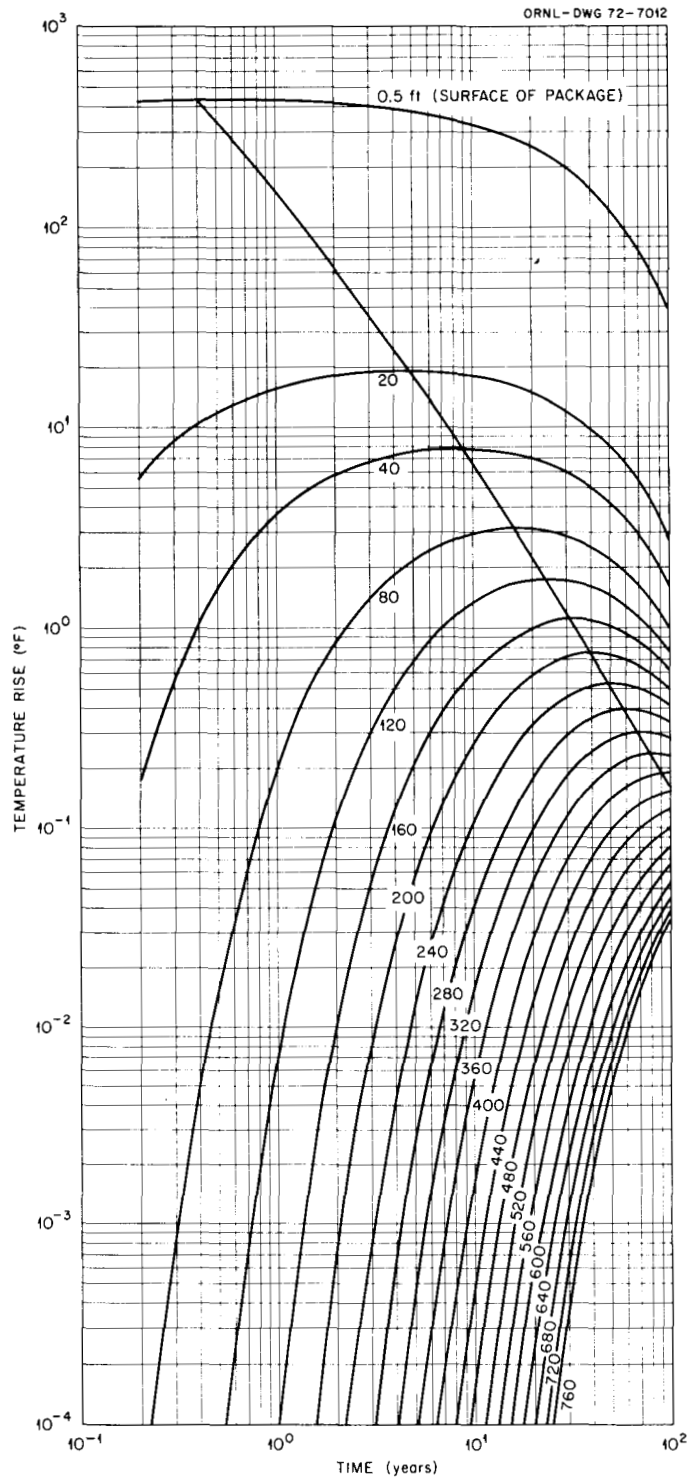


Fig. 7.18. Temperature Distribution in Space and Time for a Single High-Level Waste Package Containing 189 kg (5 kw) of 10-year-old LWR Waste Nuclides.

The temperature rise on the surface of the central package is:

$$\Delta T_{st} = \Delta T_s + 2\pi \Sigma n \Delta T_n ,$$

where

$\Delta T_{st}$  = total temperature rise on the surface of the central package,

$\Delta T_s$  = surface temperature rise with a single package,

$\Delta T_n$  = surface temperature rise with a single package at a radial distance of  $40n$  ft.

The maximum value obtained for  $T_{st}$ , using the data in Fig. 7.18, is  $464^\circ\text{F}$ .

It occurs at about 7 years.

Figure 7.18 indicates that a higher temperature could be obtained by loading each circle at the most opportune time to ensure that all of the peaks are superimposed. Suppose that the outer ten circles are loaded about 100 years before the central package is loaded, and that the other circles are loaded at the appropriate intermediate times for superposition of peaks. The resultant maximum surface temperature rise is about  $703^\circ\text{F}$ , occurring about 0.4 year after the final package (central package) has been buried. Of course, such a burial scheme is not realistic, although it does illustrate the potential effect of phasing.

An actual loading sequence being considered for the Repository results in a 10-year lapse between burial in adjacent sections. Suppose that the distance between the back ends of rooms of the two sections is about 40 ft, that the minimum distance between packages in the two sections is 40 ft, and that the spacing within a section is also 40 ft. Further, suppose that both sections are loaded instantaneously but one is loaded 10 years prior to the other. Again, using the circular array, the number of packages in the first section that is a radial distance of

40n ft from a centrally-located package at the closest edge of the second section is  $\pi n-1$ . The corresponding number in the second section is  $\pi n+1$ . Using the superposition technique, the maximum surface temperature rise is found to be 500°F. Thus, the error in assuming instantaneous loading is  $500 - 464 = 36^\circ\text{F}$ . If the minimum distance between packages in adjacent sections is 80 ft rather than 40 ft, but the spacing within each section is still 40 ft, the error is only 9°F. These results indicate that maximum temperatures can be accurately calculated for normal operation of the Repository, assuming that all waste is buried at the same time. This is fortunate since three-dimensional models, which are required for much of the Repository analysis, would be impractical (considering computer time) if loading sequence had to be considered. For some unusual (or at least unanticipated) cases, the sequence may need to be considered. In that event, the single-package superposition model can be used to obtain correction factors to be applied to the instantaneous-loading results, or to determine spacings that will minimize the effect.

## 8. REFERENCES

1. R. L. Bradshaw et al., Evaluation of Ultimate Disposal Methods for Liquid and Solid Radioactive Wastes: VI. Disposal of Solid Wastes in Salt Formations, ORNL-3358 (Rev.) (March 1969).
2. R. D. Cheverton and W. D. Turner, Thermal Analysis of the National Radioactive Waste Repository: Progress Through June 1971, ORNL-4726 (December 1971).
3. Staff of the Oak Ridge National Laboratory, Siting of Fuel Reprocessing Plants and Waste Management Facilities, ORNL-4451 (July 1970).
4. R. S. Dillon, J. J. Perona, and J. O. Blomeke, A Model for the Economic Analysis of High-Level Radioactive Waste Management, ORNL-4633 (November 1971).
5. J. Douglass, "Alternating Direction Methods for Three Space Variables," Numer. Math. 4, 41 (1962).
6. M. J. Bell, Radiation Properties of Spent Plutonium Fuels, ORNL-TM-3641 (January 1972).
7. J. O. Blomeke and J. J. Perona, Storage, Shipment and Disposal of Spent Fuel Cladding, ORNL-TM-3650 (January 1972).
8. H. W. Godbee and J. P. Nichols, Sources of Transuranium Solid Waste and Their Influence on the Proposed National Radioactive Waste Repository, ORNL-TM-3277 (January 1971).
9. J. H. Sass, letter to W. C. McClain, Mar. 22, 1971.
10. D. L. McElroy and T. G. Godfrey, ORNL internal memorandum, November 1971.
11. K. J. Schneider, "Solidification and Disposal of High-Level Radioactive Wastes in the United States," Reactor Technol. 13 (No. 4) (Winter 1970-71).
12. R. L. Bradshaw and W. C. McClain, Project Salt Vault: A Demonstration of the Disposal of High Activity Solidified Wastes in Underground Salt Mines, ORNL-4555 (April 1971).
13. R. S. Dillon, Steady State Surface Temperature Calculation of Waste Cylinder Standing in Air, internal memorandum to J. O. Blomeke, Dec. 3, 1970.
14. R. D. Cheverton, unpublished thermal analysis of transporter, February 1972.

15. E. D. Arnold, H. F. Soard, and J. O. Blomeke, ORNL internal memorandum, January 1971.
16. J. O. Blomeke, personal communication, December 1971.
17. W. H. McAdams, Heat Transmission, 2d ed., McGraw-Hill, New York, 1942.
18. J. O. Blomeke and J. J. Perona, Storage, Shipment and Disposal of Spent Fuel Cladding, ORNL-TM-3650 (January 1972).
19. Radioactive Waste Repository Project: Technical Status Report for Period Ending September 30, 1971, ORNL-4751 (December 1971), p. 135.

ORNL-4789

UC-70 - Waste Disposal and Processing

## INTERNAL DISTRIBUTION

- |                                     |                       |
|-------------------------------------|-----------------------|
| 1-3. Central Research Library       | 86. F. Gera           |
| 4. ORNL - Y-12 Technical Library    | 87. H. W. Godbee      |
| Document Reference Section          | 88. T. G. Godfrey     |
| 5-29. Laboratory Records Department | 89. W. R. Grimes      |
| 30. Laboratory Records, ORNL R.C.   | 90. R. F. Hibbs       |
| 31. S. E. Beall                     | 91. J. M. Holmes      |
| 32. D. S. Billington                | 92. G. H. Jenks       |
| 33-34. J. O. Blomeke                | 93. W. H. Jordan      |
| 35-44. A. L. Boch                   | 94. M. J. Ketelle     |
| 45. E. G. Bohlmann                  | 95. E. Lamb           |
| 46. C. D. Bopp                      | 96. T. F. Lomenick    |
| 47. C. J. Borkowski                 | 97. R. A. Lorenz      |
| 48. B. F. Bottenfield               | 98. A. P. Malinauskas |
| 49. G. E. Boyd                      | 99. W. C. McClain     |
| 60. A. A. Brooks                    | 100. D. E. McElroy    |
| 61. H. P. Carter                    | 101. J. P. Nichols    |
| 62-76. R. D. Cheverton              | 102. J. J. Perona     |
| 77. H. C. Claiborne                 | 103. A. M. Perry      |
| 78. J. S. Crowell                   | 104. G. W. Renfro     |
| 79. F. L. Culler                    | 105. G. Samuels       |
| 80. R. C. Dahlman                   | 106. M. Siman-Tov     |
| 81. W. de Laguna                    | 107. E. Sonder        |
| 82. F. M. Empson                    | 108. D. B. Trauger    |
| 83. R. B. Evans III                 | 109. W. D. Turner     |
| 84. D. E. Ferguson                  | 110. A. M. Weinberg   |
| 85. E. J. Frederick                 |                       |

## EXTERNAL DISTRIBUTION

- U.S. Atomic Energy Commission, Washington, D.C. 20545
- 111. C. B. Bartlett, Division of Waste Management and Transportation
  - 112. O. P. Gormley, Division of Waste Management and Transportation
  - 113. A. F. Perge, Division of Waste Management and Transportation
  - 114. F. K. Pittman, Division of Waste Management and Transportation
  - 115. R. W. Ramsey, Division of Waste Management and Transportation
  - 116. R. M. Richardson, Division of Waste Management and Transportation
  - 117. Milton Shaw, Division of Reactor Development and Technology
  - 118. W. A. Burns, Advisory Committee on Reactor Safeguards
- U.S. Atomic Energy Commission, Oak Ridge Operations Office, Oak Ridge, Tennessee 37830
- 119. R. L. Egli, Research and Technical Support Division
  - 120. E. F. Newman, Engineering Division
  - 121-125. B. M. Robinson, Research and Technical Support Division
  - 126. Research and Technical Support Division

- U.S. Atomic Energy Commission, Oak Ridge, Tennessee 37830  
127. D. F. Cope, RDT Site Office (ORNL)
- Argonne National Laboratory, Chemistry Division. Building 200, Argonne,  
Illinois 60439  
128. J. J. Katz
- Atlantic Richfield Hanford Company, P.O. Box 250, Richland, Washington  
99352  
129. M. J. Szulinski
- Battelle Memorial Institute, Pacific Northwest Laboratory, P.O. Box 999,  
Richland, Washington 99352  
130. A. M. Platt
- 1005 Berkshire Road, Ann Arbor, Michigan 48104  
131. K. K. Landes
- University of California at Los Angeles, Institute of Geophysics and  
Planetary Physics, Los Angeles, California 90024  
132. George Kennedy
- University of California, Department of Geological Sciences, Riverside,  
California 92502  
133. R. W. Rex
- E. I. du Pont de Nemours & Company, Savannah River Operations Office,  
Augusta, Georgia 30900  
134. C. H. Ice
- General Electric Company, Reactor and Fuels Reprocessing Department, 175  
Curtner Avenue, San Jose, California 95100  
135. R. B. Richards
- Illinois State Geological Survey, Natural Resources Building, Urbana,  
Illinois 61801  
136. J. C. Frye
- Kaiser Engineers, Kaiser Center, Oakland, California 94604  
137. F. H. Harris  
138. A. L. Lindsay
- Kansas State Department of Health, State Office Building, Topeka,  
Kansas 66612  
139. B. F. Latta  
140. Blaine Murray  
141. R. C. Will
- University of Kansas, Department of Chemical and Petroleum Engineering,  
Lawrence, Kansas 66044  
142. G. P. Willhite
- University of Kansas, Department of Geology, Lawrence, Kansas 66044  
143. E. E. Angino  
144. L. F. Dellwig  
145. E. L. Zeller

University of Kansas, State Geological Survey, Lawrence, Kansas 66044  
146. W. W. Hambleton

Los Alamos Scientific Laboratory, P.O. Box 1663, Los Alamos, New Mexico 87544

147. R. J. Dietz

148. G. L. Voelz

Massachusetts Institute of Technology, 138 Albany Street, Cambridge, Massachusetts 02139

149. E. A. Mason

University of Minnesota, Department of Civil and Mineral Engineering, Minneapolis, Minnesota 55455

150. S. L. Crouch

151. Charles Fairhurst

University of Missouri, Columbia, Missouri 65201

152. Walter Meyer

University of Missouri at Kansas City, Department of Geology, Kansas City, Missouri 64141

153. E. D. Goebel

New Mexico Environmental Improvement Agency, State Capitol Building, Santa Fe, New Mexico 87501

154. Aaron Bond

New Mexico Institute of Mining and Technology, Socorro, New Mexico 67801

155. G. K. Billings

New Mexico State Bureau of Mines and Mineral Resources, Socorro, New Mexico 87801

156. D. H. Baker

RE/SPEC Inc., P.O. Box 725, Rapid City, South Dakota 57701

157. P. F. Gnirk

Route 2, Salina, Kansas 67401

158. O. S. Fent

3 Sonoma Lane, Carmel, California 93921

159. A. M. Piper

State Planning Office, Santa Fe, New Mexico 87501

160. D. W. King, State Planning Officer

University of Tennessee, Department of Geology, Knoxville, Tennessee 37916

161. O. C. Kopp

Union Carbide Corporation, New York, New York 10017

162. J. A. Swartout

U.S. Department of the Interior, Geological Survey, Denver Federal Center, Denver, Colorado 80225

163. W. S. Twenhofel, Special Projects Branch

164. Harley Barnes, Special Projects Branch

U.S. Department of the Interior, Geological Survey, Washington, D.C. 20242  
165. G. D. DeBuchanne, Office of Radiohydrology, Water Resources  
Division

U.S. Department of the Interior, Office of Deputy Director for Health and  
Safety, Washington, D.C. 20240  
166. B. F. Grant

U.S. Geological Survey, Earthquake Research Center, Menlo Park, California  
94025  
167. C. B. Raleigh

Walters Drilling Company, 400 Insurance Building, Wichita, Kansas 67202  
168. R. F. Walters

Westinghouse Electronic Corporation, Advanced Reactors Division, P.O. Box  
158, Madison, Pennsylvania 15663  
169. Peter Murray

TID-4500 Category Distribution  
170-344. Given distribution as shown in TID-4500 under Waste Disposal and  
Processing category (25 copies - NTIS)